Journal of
Medicinal Chemistry

Article

Discovery of highly selective inhibitors of calmodulin-dependent kinases that restore insulin sensitivity in the diet-induced obese *in vivo* mouse model.

Christophe Fromont, Alessio Atzori, Divneet Kaur, Lubna Hashmi, Graziella Greco, Alejandro Cabanillas, Huy Van Nguyen, D. Heulyn Jones, Miguel Garzón, Ana Varela, Brett Stevenson, Greg Iacobini, Marc Lenoir, Sundaresan Rajesh, Clare Box, Jitendra Kumar, Paige Grant, Vera Novitskaia, Juliet Morgan, Fiona Sorrell, Clara Redondo, Andreas Kramer, C. John Harris, Brendan Leighton, Steven Vickers, Sharon Cheetham, Colin Kenyon, Anna M. Grabowska, Michael Overduin, Fedor Berditchevski, Chris J Weston, Stefan Knapp, Peter M. Fischer, and Sam Butterworth

J. Med. Chem., **Just Accepted Manuscript** • DOI: 10.1021/acs.jmedchem.9b01803 • Publication Date (Web): 20 May 2020

Just Accepted

is published by the American Chemical Society. 1155 Sixteenth Street N.W., Washington, DC 20036

	Cheetham, Sharon; RenaSci Ltd Kenyon, Colin; Stellenbosch University, DST/NRF Centre of Excellence for Biomedical Tuberculosis Research, SAMRC Centre for Molecular and Cellular Biology Grabowska, Anna; University of Nottingham, Division of Pre-Clinical Oncology Overduin, Michael; University of Alberta, Department of Biochemistry Berditchevski, Fedor; University of Birmingham, Institute of Cancer and Genomic Sciences, College of Medical and Dental Sciences Weston, Chris; University of Birmingham, Institute of Immunology and Immunotherapy, College of Medical and Dental Sciences Knapp, Stefan; Goethe-Universitat Frankfurt am Main, Instutute of Pharmaceutical Chemistry Fischer, Peter; University of Nottingham Centre for Biomolecular Sciences, School of Pharmacy Butterworth, Sam; University of Manchester, Pharmacy and Optometry

Discovery of highly selective inhibitors of calmodulin-dependent kinases that restore insulin sensitivity in the diet-induced obese *in vivo* mouse model.

Authors

Christophe Fromont,[§] Alessio Atzori, [§] Divneet Kaur,[§] Lubna Hashmi,[§] Graziella Greco,[¶] Alejandro Cabanillas,[¶] Huy Van Nguyen,[¶] D. Heulyn Jones,[#] Miguel Garzón,[#] Ana Varela,[#] Brett Stevenson,[+] Greg P. Iacobini,[+] Marc Lenoir,[Φ] Sundaresan Rajesh,[Φ] Clare Box,[Φ] Jitendra Kumar,[ϒ] Paige Grant,[ϒ] Vera Novitskaya,[Φ] Juliet Morgan,[+] Fiona J. Sorrell,[ε] Clara Redondo,[ε] Andreas Kramer,[Ψ] C. John Harris,[ρ] Brendan Leighton,[Ω] Steven P. Vickers,[ϑ] Sharon C. Cheetham,[ϑ] Colin Kenyon,[ς] Anna M. Grabowska,[ϖ] Michael Overduin,[ϒ] Fedor Berditchevski,[Φ] Chris J. Weston,[λ] Stefan Knapp,[Ψ] Peter M. Fischer[§] and Sam Butterworth[#]*

Affiliations

[#]Division of Pharmacy and Optometry, School of Health Sciences, Manchester Academic Health Sciences Centre, University of Manchester, Manchester, M13 9PL, UK.

[§]Centre for Biomolecular Sciences and School of Pharmacy, University of Nottingham, Nottingham NG7 2RD, UK.

[¶]School of Pharmacy, College of Medical and Dental Sciences, University of Birmingham, Edgbaston, B15 2TT, UK.

[Φ]Institute of Cancer and Genomic Sciences, University of Birmingham, Edgbaston, Birmingham, B15 2TT, UK.

[+]Sygnature Discovery, BioCity, Pennyfoot Street, Nottingham, NG1 1GF, UK.

[γ]Department of Biochemistry, University of Alberta, Edmonton, Alberta T6G 2H7, Canada.

[ε]Structural Genomics Consortium and Target Discovery Institute, Nuffield Department of Clinical Medicine, University of Oxford, Old Road Campus Research Building, Oxford OX3 7DQ, UK.

[Ψ]Structural Genomics Consortium and Buchmann Institute for Molecular Life Sciences, Institute for Pharmaceutical Chemistry, Johann Wolfgang Goethe-University, Max-von-Laue-Straße 9, 60438 Frankfurt am Main, Germany.

[ϑ]RenaSci Limited, BioCity, Pennyfoot Street, Nottingham, NG1 1GF, UK.

[ρ]CJH Consultants, Ford Cottage, South Weirs, Burley Road, Brockenhurst, Hants, SO42 7UQ, UK.

[Ω]The Research Network, IPC 600 Discovery Park, Ramsgate Road, Sandwich CT13 9NJ.

[ς]DST/NRF Centre of Excellence for Biomedical Tuberculosis Research, SAMRC Centre for Molecular and Cellular Biology, Division of Molecular Biology and Human Genetics, Faculty of Medicine and Health Sciences, Stellenbosch University, Cape Town 8000, South Africa

[ϖ]Ex Vivo Cancer Pharmacology Centre of Excellence, Cancer Biology, Division of Cancer and Stem Cells, School of Medicine, University of Nottingham, Nottingham NG7 2RD, UK.

[λ]Centre for Liver Research, Institute of Immunology and Immunotherapy, University of Birmingham, Birmingham, B15 2TT, UK, and NIHR Birmingham Biomedical Research Centre, University Hospitals Birmingham NHS Foundation Trust and University of Birmingham, B15 2TT, UK

ABSTRACT

Polymorphisms in the region of the calmodulin-dependent kinase isoform D (CaMK1D) gene are associated with increased incidence of diabetes, with the most common polymorphism resulting in increased recognition by transcription factors and increased protein expression. While reducing CaMK1D expression has a potentially beneficial effect on glucose processing in human hepatocytes, there are no known selective inhibitors of CaMK1 kinases that can be used to validate or translate these findings. Here we describe the development of a series of potent, selective and drug-like CaMK1 inhibitors that are able to provide significant free target cover in mouse models and are therefore useful as *in vivo* tool compounds. Our results show that a lead compound from this series improves insulin sensitivity and glucose control in the diet-induced obesity mouse model after both acute and chronic administration, providing the first *in vivo* validation of CaMK1D as a target for diabetes therapeutics.

INTRODUCTION

The CaMK1 family of calmodulin-dependent kinases are widely expressed including in hepatocytes, endothelia, immune cells, and the CNS.[1,2] There are four CaMK1 isoforms with high similarity in the kinase domain, especially the ATP binding site, but which differ in their overall structure and tissue distribution.

Single-nucleotide polymorphisms in the CaMK1D locus are associated with increased incidence of diabetes in a large number of genome-wide association studies (GWAS).[3–6] While these variations are non-coding it has been demonstrated that the diabetes-associated polymorphism rs11257655 increases FOXA1 transcription factor binding and thereby increases CaMK1D protein expression in multiple cell models.[7]

A direct role for CaMK1D in glucose processing has been observed following knock-down of commonly observed GWAS-identified proteins in primary human hepatocytes.[8] In this model treatment with CaMK1D siRNA results in loss of nuclear translocation of the established diabetes target CRTC2/TORC2[9–11] and is associated with decreased gluconeogenesis and increased glycogen deposition.

Increased CaMK1D expression is also implicated in triple-negative breast cancer (TNBC). Large-scale genomic/transcriptomic analyses of breast tumours indicate that gains at the 10p13 locus, which spans the CaMK1D gene, are observed in 80% of TNBC tumours[12] with high occurrence in estrogen receptor-negative and TNBC tumours of younger patients.[13] In a separate study, biopsies from 172 breast cancer patients showed significant gains at the 10p13 locus among basal-like tumours, leading to CaMK1D over-expression at transcriptional and protein level.[14] When expressed in non-tumourigenic mammary epithelial cells (MCF10A), CaMK1D was found to lead to transformation, increasing proliferation and inducing a mesenchymal-like phenotype.[14] Mouse models also corroborate the effect of overexpressing CaMK1D on altered cell proliferation and apoptosis.[15]

Despite the emergence of CaMK1D as a potentially important therapeutic target, there are no known selective CaMK1 inhibitors. We therefore sought to develop potent and selective inhibitors of this class of kinases for use in target validation experiments, ahead of further translational studies.

RESULTS AND DISCUSSION

Compound **1** and derivatives thereof have received significant attention as inhibitors of spleen tyrosine kinase (SYK) and may have utility in the treatment of autoimmune disease or lymphomas.[16–19] Previously published selectivity data shows compound **1** to have inhibitory activity against CaMK1D[20] and as such we selected this as the basis for a structure-based drug discovery campaign, with the aim of improving the potency and selectivity of compounds from this series towards CaMK1D. We initially examined the compound-induced shift in the thermal denaturation midpoint (T_m) of a small panel of kinases, in order to allow rapid quantification of the binding to both CaMK1D and off-target kinases (Table 1). Initial chemical efforts focussed on alterations in the primary amide and amine regions, resulting in compounds **2**-**6**, which demonstrate comparatively steep structure activity relationships when either the primary amide or primary amine are substituted. Substitution of the secondary amine to give compound **3** is well tolerated and results in an apparent improvement in kinase selectivity, with further derivatisation leading to compound **6**, which demonstrated a higher T_m shift against CaMK1D and improved selectivity relative to earlier compounds. Separation of the enantiomers of this compound led to compounds **7** and **8**, the latter of which has previously been reported as a SYK inhibitor[17] but has higher activity against CaMK1D than its enantiomer and demonstrates a more favourable activity profile relative to compounds **1** and **2** in both T_m and enzymatic assays.

Table 1. Structure-Activity Relationships of Pyrimidine Amides.

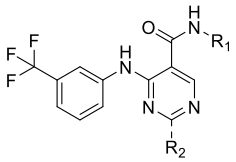

Compound	R_1	R_2	T_m shift (°C)						IC_{50} (μM)	
			CaMK1D	SYK	DAPK3	GSK3β	CaMK4	DCLK1	CaMK1D	SYK
1	H	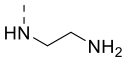	5.44 (0.58)	7.51 (0.09)	4.05 (0.29)	3.4 (0.44)	1.34 (0.28)	0.11 (0.25)	0.456[a] 0.432 (0.084)	0.007[a]
2	Me	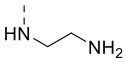	0.12 (0.3)	-	1.36 (0.16)	-0.27 (0.39)	-0.18 (0.18)	-0.53 (0.15)	-	-
3	H	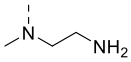	7.35 (0.4)	5.13 (0.17)	4.48 (0.13)	0.84 (0.13)	2.13 (0.21)	0.10 (0.07)	0.851 (0.160)	-
4	H	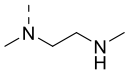	2.43 (0.08)	-	2.70 (0.27)	0.70 (0.16)	3.36 (0.08)	0.11 (0.14)	3.49[a]	-
5	H	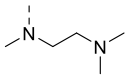	4.68 (0.11)	-	3.45 (0.31)	0.76 (0.19)	2.21 (0.1)	0.08 (0.23)	-	-
6	H	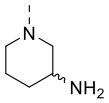	9.84 (0.17)	8.59 (0.34)	6.69 (0.11)	2.31 (0.13)	4.94 (0.08)	1.08 (0.04)	0.485 (0.017)	-
7	H	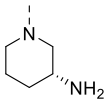	6.84 (0.07)	6.82 (0.39)	4.63 (0.03)	1.70 (0.12)	3.36 (0.14)	0.95 (0.05)	1.35 (0.018)	-
8	H	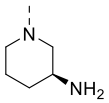	10.5 (0.04)	9.05 (0.36)	7.01 (0.01)	2.50 (0.16)	5.09 (0.15)	1.1 (0.08)	0.179[a] 0.186 (0.027)	0.087[a]

All data represents mean of at least n=3 independent experiments with standard deviation in parentheses, except; [a] Compounds tested at Reaction Biology n=1.

Based on these results we evaluated the pan-kinome selectivity of **8** in a competitive binding assay at 1 μM, which demonstrated a somewhat targeted profile. CaMK1D and SYK are amongst the 11 wild-type kinases inhibited by >90% in this format,

supported by subsequent enzymatic selectivity data against selected targets (Fig. 1 and SI).

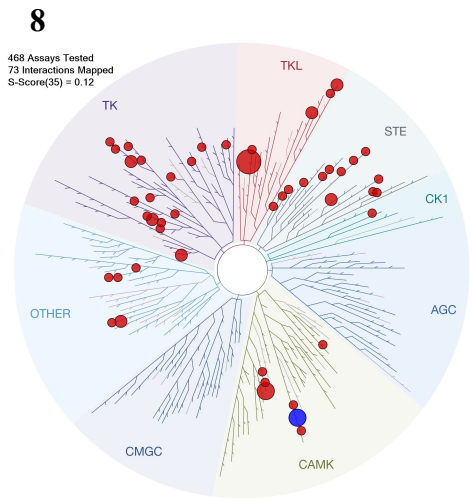

Kinase	% residual probe binding at 1 μM[a]	Enzyme IC_{50} (μM)[b]
RIPK4	0.9	0.092
CaMK1D	2.0	0.179
PIM1	2.7	0.053
TAK1	5.7	0.356
CK2a	6.5	9.131
MEK5	7.3	0.240
PIP5K1C	8.1	-
CSF1R	8.6	0.168
MLK3	8.9	0.052
BLK	9.5	0.057
SYK	9.6	0.087

Figure 1. Selectivity data against selected wild-type kinases for compound **8**

[a]Compounds tested at Eurofins DiscoverX, n=1. [b]Compounds tested at Reaction Biology, n=1.

As expected the CaMK1D-bound crystal structure of compound **8** shows the compound binds at the ATP binding site in a type-1 fashion. A comparison of the binding mode of related compounds in SYK (e.g. PDB: 4RX9) demonstrated a slight shift in binding mode resulting from differences in the conformation of the loop at residues 163-165 (corresponding to 510-512 in SYK) as well as a flip in the orientation of the aniline *meta*-substituent in CaMK1D to occupy a pocket adjacent to L100 at the edge of the hinge region. The L100 pocket appears significantly larger in CaMK1D than the majority of the observed off-targets where structural data was available. In addition, the second *meta* region that is not utilised by **8** is close to the potentially flexible side chain of E105. We hypothesised that flipping of the

orientation of the aniline allows the ligand to avoid the L100 pocket when binding to some off-target kinases. This led to the design of compound **9** that removes this ambiguous binding mode by occupying both the L100 and E105 regions.

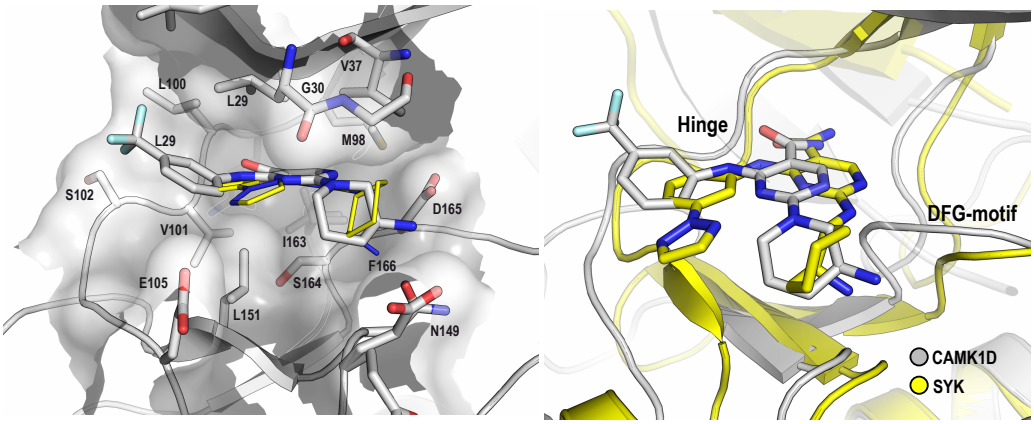

Figure 2. Compound **8** bound to CaMK1D (6T6F, white) and overlay with related SYK structure (4RX9, yellow). Important residues and inhibitors are shown in stick representation. For better visibility the P-Loop has been made transparent.

This bis-*meta* substitution pattern was well tolerated by CaMK1D when assessed by T_m shift and resulted in a significant decrease in the binding to off-targets including SYK (Table 2). Further SAR studies identified that a wide range of functional groups can be tolerated at the L100 pocket, with introduction of groups with a wide range of lipophilicity and bonding potential able to maintain or even enhance binding and selectivity (Table 2).

Table 2. Effects of varying aniline substitution on potency/selectivity.

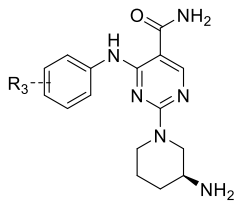

Compound	R_3	T_m shift (°C)						Enzyme IC_{50} (μM)
		CaMK1D	SYK	DAPK1	CK2a	ABL	PIM1	CaMK1D
8	3-CF_3	10.5 (0.04)	9.05 (0.36)	5.92 (0.45)	3.77 (0.12)	5.02 (0.36)	8.32 (0.28)	0.186 (0.027)
9	3,5-diCF_3	13.3 (0.09)	4.13 (0.57)	6.07 (0.06)	5.89 (0.1)	3.88 (0.24)	3.98 (0.05)	0.455 (0.451)
10	3-*t*Bu	9.61 (0.16)	4.58[a] (0.33)	3.02 (0.09)	3.02 (0.56)	2.27 (0.22)	2.09 (0.44)	0.277[b] (0.053)
11	3-SO_2Me	7.85 (0.09)	5.23 (0.18)	4.21 (0.09)	5.11 (0.02)	5.33 (0.09)	1.78 (0.65)	0.101 (0.07)
12	3-Ph	11.9 (0.26)	9.32 (0.29)	4.81 (0.11)	3.79 (0.01)	4.5 (0.26)	4.96 (0.06)	0.047 (0.026)
13	3-(2-cyano*i*Pr)	7.76 (0.24)	5.00 (0.28)	3.32 (0.39)	9.51 (0.19)	2.85 (0.28)	1.3 (0.2)	0.096 (0.05)

All data represents mean of at least n=3 independent experiments with standard deviation in parentheses. [a]Measured on racemic compound. [b]n=2.

The binding affinity and selectivity for CaMK1D were further improved by combining these structural features in symmetrical and unsymmetrical bis-meta substituted anilines, especially those containing substituents that place electron density above and below the aniline ring plane. The clearest example of this is compound **14**, which is too lipophilic to be a useful lead compound but nonetheless exhibits a very high T_m shift with CaMK1D and negligible off target binding. Evaluation of **14** in pan-kinome selectivity assay reveals highly specific binding to CaMK1D and the closely related CaMK1A and CaMK1B, again supported by enzymatic evaluation (Figure 3 and SI).

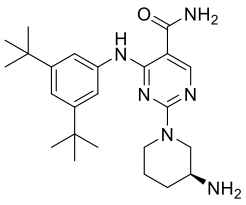

14

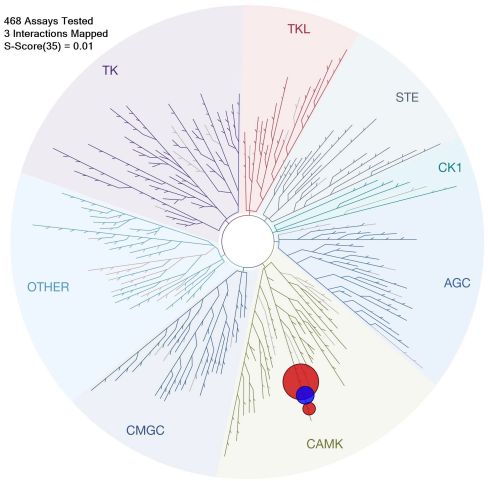

Kinase	T_m shift (°C)	% residual probe binding at 1 μM[a]	Enzyme IC_{50} (μM)[b]
CaMK1D	12.4 (0.07)	1.4	0.399
CaMK1B	-	0.0	-
CaMK1A	-	8.8	-
DAPK1	1.13 (0.03)	81	-
CK2a	-0.03 (0.08)	100	-
PIM1	-0.43 (0.93)	100	-
MEK5	-	95	>10
MLK3	-	77	>10
SYK	0.37 (0.27)	82	-

Figure 3. Selectivity data against selected wild-type kinases for compound **14**. T_m shift data represents mean of at least n=3 independent experiments with standard deviation in parentheses, see supporting information for experimental details. [a]Compounds tested at Eurofins DiscoverX, n=1. [b]Compounds tested at Reaction Biology, n=1.

Our hypothesis is that the disconnect between the apparent high binding of **14** observed by T_m shift and the competitive binding assay at DiscoveRx, compared to the lower activity in competitive inhibition assays, relate to it's poor physiochemical properties, which may lead to compound losses during serial dilution.

Despite the issues with properties in this specific example, we believed **14** demonstrated the potential to achieve high selectivity in this series and therefore sought to combine this selectivity with improved potency and physical properties by exploiting the wide SAR scope at the aniline *meta* positions. Subsequent evaluation of a wide range of aniline substituents generally validated our hypothesis that 'bulky' substituents are favoured for both potency and selectivity.

This work led to compounds **15-18,** which show good binding and selectivity in both T_m and enzymatic assays. Selected compounds were assessed for their ability to inhibit auto-phosphorylation of CaMK1D at activation loop residues serine 179 and threonine 180 in over-expressing MDA-MB-231 cells. This data demonstrated that the inhibitors have limited cell drop-off for compounds with no additional H-bond donors or basic centres (Table 3). Pan-kinome screening data on **18** shows the high selectivity of **14** can be maintained in compounds with more favourable physicochemical properties, with enzymatic data on identified off-targets demonstrating >150-fold greater activity vs CaMK1D than all non-CaMK1 kinases.

The *in vitro* pharmacokinetic profile of **18** reveals generally favourable properties with high solubility, low metabolism and moderately high plasma protein binding (PPB), but low permeability with some evidence of efflux in the CaCo2 model (Table 5). This low permeability does not appear to impact on either cellular activity or oral pharmacokinetics, where **18** shows good bioavailability in mice and rats despite moderately high clearance.

Table 3. Effects of varying substitution of bis-*meta* substituted anilines on potency and selectivity.

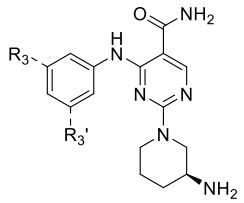

Compound	R_3	R_3'	T_m shift (°C) CaMK1D	SYK	DAPK1	CK2a	ABL	PIM1	CaMK1D IC_{50} (μM) enzyme	cell
15	*i*Pr	*i*Pr	11.9 (0.15)	8.20 (0.37)	4.65 (0.19)	4.05 (0.07)	5.95 (0.17)	0.62 (0.32)	0.115 (0.051)	0.285[a] (0.013)
16	*t*Bu	SO_2Me	11.8 (0.25)	0.87 (0.38)	3.83 (0.19)	1.85 (0.16)	1.09 (0.06)	0.94 (0.46)	0.027 (0.005)	0.028[a] (0.011)
17	2-cyano-*i*Pr	Ph	15.9 (0.13)	-	4.8 (0.2)	-0.21 (0.37)	1.95 (0.02)	1.11 (0.14)	0.022 (0.009)	0.019[a] (0.001)
18	2-cyano-*i*Pr	2-cyano-*i*Pr	11.5 (0.17)	-	3.46 (0.23)	0.56 (0.16)	0.27 (0.16)	0.81 (0.27)	0.031 (0.003)	0.008 (0.002)

All data represents mean of at least n=3 independent experiments with standard deviation in parentheses, except; [a]n=2.

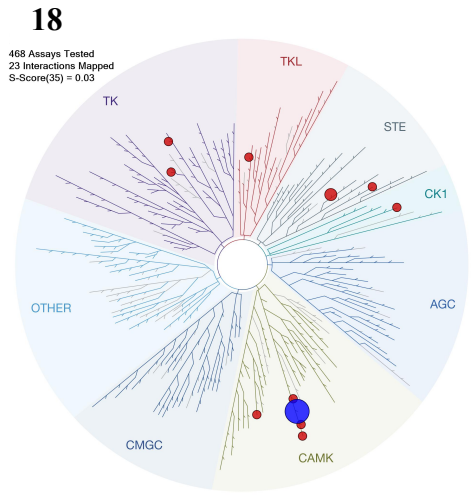

Kinase	% residual probe binding at 1 μM[a]	IC_{50} (μM)[b]
CaMK1D	0.9	0.026[c]
CaMK1B	15	0.011 (<0.001)
CaMK1A	16	0.002 (0.001)
PIP5K1C	3.0	7.12[c]
MEK5	9.8	7.68 (0.547)
MLK3	95	7.86 (4.20)

Figure 4. Selectivity data against selected wild-type kinases for compound **18**. [a]Compounds tested at Eurofins DiscoverX, n=1. [b]Compounds tested at Reaction

Biology, n=2 independent experiments with standard deviation in parentheses except [c]n=1.

The oral pharmacokinetic profile of **18** in mice scaled well at doses up to 100 mg/kg, and the PPB-adjusted cover over cellular IC_{50} observed suggested that this compound may be suitable for *in vivo* target validation studies (Figure 5).

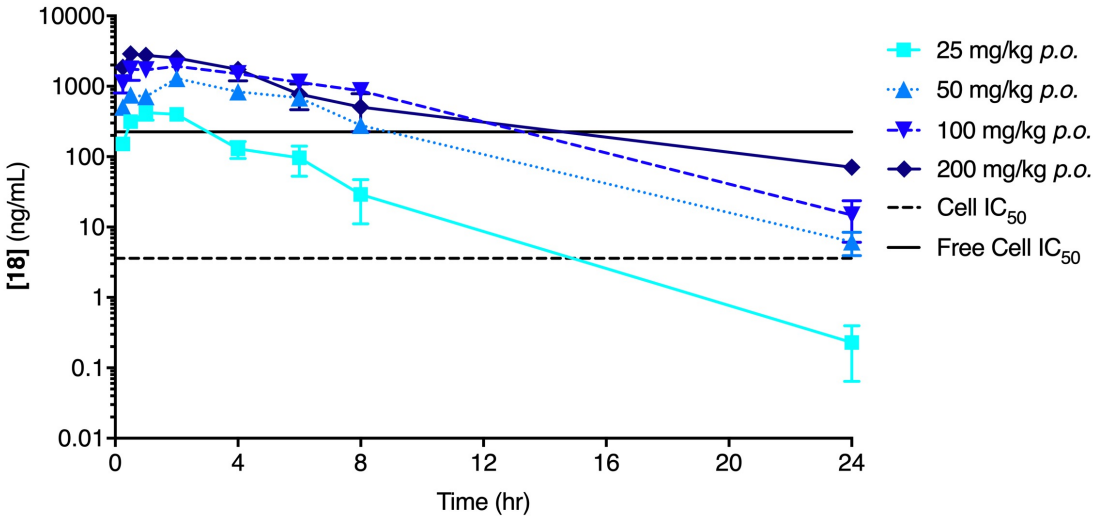

		Mouse					Rat	
Route	*i.v.*	*p.o.*	*p.o.*	*p.o.*	*p.o.*	*p.o.*	*i.v.*	*p.o.*
Dose (mg/kg)	2	10	25	50	100	200	1	7
%F	-	41	37	88	94	45	-	73
CL (mL/min/kg)	88	-	-	-	-	-	125	-
AUC (0->inf, ng.h/mL)	387	790	1775	8497	18305	17522	134	684
C_{max} (ng/mL)	747	196	453	1294	2221	3057	133	136
$t_{1/2}$ (h)	2.3	1.2	1.7	2.7	2.8	4.7	6.2	3.3
V_{ss} (L/kg)	4.9		-	-	-	-	40.3	-

Figure 5. *In vivo* pharmacokinetic profile of **18** in male CD-1 mice (25-40 g) and male Crl:CD Sprague Dawley rats (250-400 g) dosed in 10% DMSO/90%

hydroxypropyl-beta-cyclodextrin (20% w/v), n=3 per group. Free cell IC_{50} was calculated by dividing measured cellular IC_{50} by free fraction in mouse plasma.

In order to improve the potential utility of these compounds, we sought to identify a lead compound with improved potency and reduced clearance in order to allow for greater cover in *in vivo* experiments at reduced doses. In common with **18**, a large number of compounds from this series demonstrated high solubility, low A-B/high B-A CaCo2 permeability and moderate to low metabolism in mouse microsome and hepatocyte assays. However, the *in vivo* clearance of the compounds was often greater than estimated liver blood flow, suggesting that hepatic metabolism is not the key driver of clearance in mouse.

A more detailed evaluation of the *in vivo* pharmacokinetics of **18** revealed a similar picture. Despite its high *in vivo* clearance, metabolite identification studies on rat *ex vivo* plasma samples reveals only low levels of metabolites, resulting from oxidation, acetylation or amide hydrolysis (potentially subsequent to acetylation), while analysis of urine collected from **18** dosed rats reveals renal excretion of unchanged drug at least partially contributes to clearance.

Despite the poor predictivity of the *in vitro* pharmacokinetic assays, optimisation of the aniline region of the compounds was continued, relying on *in vivo* studies to distinguish compounds that showed suitable *in vitro* activity profiles. This work led to the finding that compounds containing 4-pyridyl substituents such as seen in **19** exhibited retained or enhanced activity in CaMK1D enzyme and cell assays with similar selectivity, but reduced *in vivo* clearance. Examination of the structure activity

relationships around this structural change revealed similar SAR to that observed with the anilines. Our hypothesis is that the pyridyl nitrogen is protonated in the bound state, supported by experimental data revealing that **19** is di-basic, with pKa values of 8.7 and 7.5 for the primary amine and pyridine respectively.

Table 4. Effects of introducing 2,6-di-*iso*-propylpyridine on potency and selectivity of compound **19**.

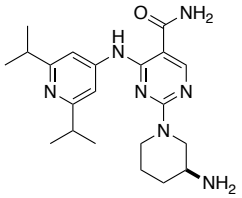

Compound	T_m shift (°C)					CaMK1D IC_{50} (μM)	
	CaMK1D	DAPK1	CK2a	ABL	PIM1	enzyme	cell
19	16.0 (0.24)	5.25 (0.02)	1.54 (0.2)	2.34 (0.06)	0.55 (0.24)	0.008 (0.001)	0.011 (0.001)

All data represents mean of at least n=3 independent experiments with standard deviation in parentheses.

The increased potency and higher *in vivo* blood concentrations seen with **19** result in significantly improved free cover over the cellular IC_{50} in mouse (Figure 7), and consistent with the low CaCo2 A-B/high B-A seen with this compound the free plasma to brain ratio is ≤0.01 at all time-points to 24 hours. The compound retains high pan-kinome selectivity, however the move to secondary (i.e. *iso*-propyl) substituents does result in a reduction in selectivity over MEK5 in both affinity and biochemical assays. These findings are reflected in the CaMK1D bound crystal

structures of compounds **18** and **19**, which show the *iso*-propyl groups in **19** occupying a low-energy conformation with the methyl groups out of the plane of the aryl ring, potentially avoiding unfavourable interactions with the protonated pyridine.

19

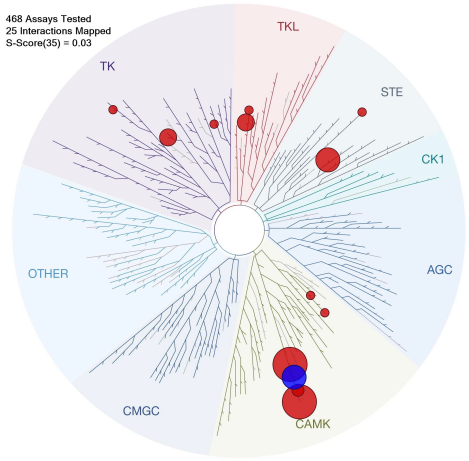

Kinase	Compound 19	
	% residual probe binding at 1 μM[a]	IC_{50} (μM)[b]
CaMK1D	0.9	0.008[c]
CaMK1B	0	0.003 (<0.001)
CaMK1A	0	0.001 (<0.001)
CaMK1G	0	0.001 (<0.001)
PIP5K1C	0	11.2 (8.50)
MEK5	0.95	0.025 (0.012)
RIPK4	4.5	5.69 (0.310)
MLK3	99	2.75 (2.05)

Figure 6. Selectivity data against selected wild-type kinases for compound **19**

[a]Compounds tested at Eurofins DiscoverX, n=1. [b]Compounds tested at Reaction Biology data, n=2 independent experiments with standard deviation in parentheses except [c]n=1.

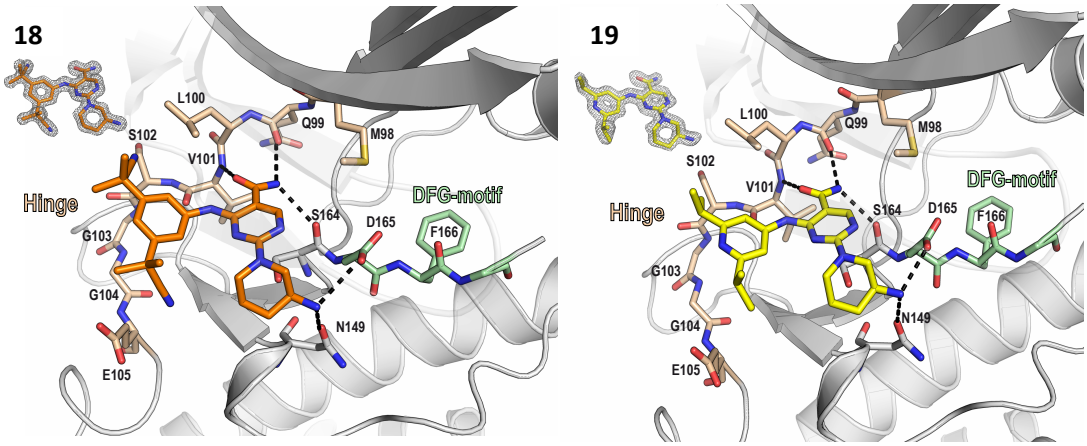

Figure 7. Comparison of the CaMK1D bound structures of compounds **18** (6T28) and **19** (6T29). CaMK1D is shown as grey cartoon representation, the hinge region is highlighted in wheat and the DFG motif in green colour. Important residues and inhibitors are shown in stick representation. For better visibility the P-Loop has been made transparent. Hydrogen bonds are indicated as black dashed lines. The inserts on the upper left of each figure show the electron density of the compounds as $2F_o$-F_c maps contoured at 1.5 σ.

Table 5. *In vitro* pharmacokinetic and toxicology profile of **18** and **19**.

	18	**19**
LogD	2.3	2.6
Solubility (μM)	52	>200
Mouse/rat/human Mics (μL/min/mg)	15 / <1 / 13	6 / 3 / 7
Mouse/rat/human Heps (μL/min/10^6 cells)	13 / 11 / -	14 / - / 19
Mouse/rat/human PPB (% bound)	98.4 / 94 / -	94 / 92 / 89
CaCo2 P_{app} (A-B x 10^{-6} cm/s)/Efflux ratio	1.1 / 13.4	0.4 / 7.9
CYP450 2C9/2C19 IC_{50} (μM)[a]	6 / 1	6 / 10
Ionworks hERG IC_{50} (μM) / ratio to cell IC_{50}	7.1 / 284	3.7 / 336

[a]CYP450 1A2, 2D6 and 3A45 IC_{50} > 20 μM for all compounds.

As expected from the high active site homology in the CaMK1 family, both **18** and **19** show limited selectivity between CaMK1A, CaMK1B, CaMK1D and CaMK1G. More detailed secondary pharmacology screening with **18** and **19** reveals some

evidence of hERG and CYP450 inhibition (Table 5) with the compounds demonstrating ~300-fold selectivity over hERG based on cellular IC_{50}.

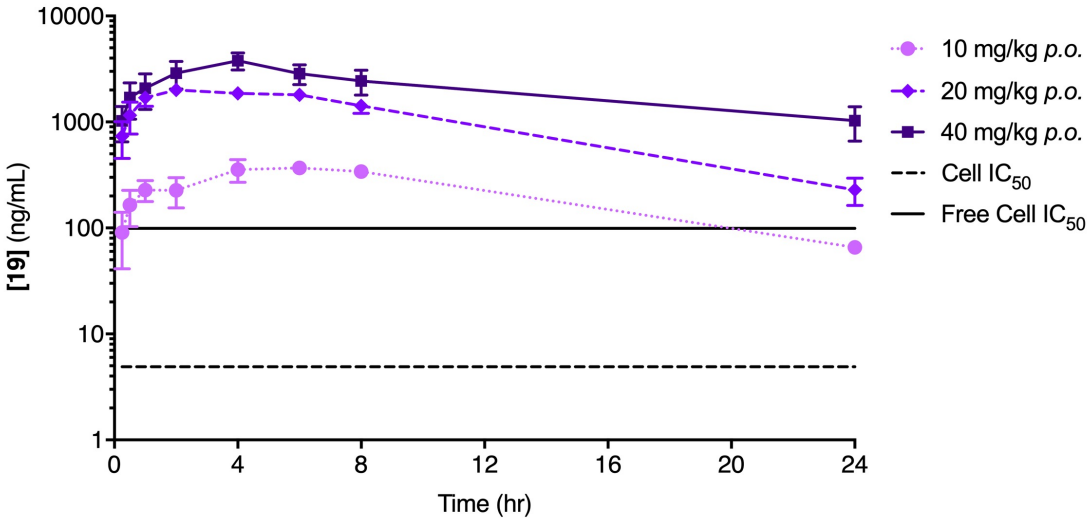

	Mouse				Rat	
Route	i.v.	p.o.	p.o.	p.o.	i.v.	p.o.
Dose (mg/kg)	2	10	20	40	2	10
F%	-	44	118	100	-	67.5
CL (mL/min/kg)	13.7	-	-	-	36.5	-
AUC (0-inf, ng.hr/mL)	2454	5408	28923	49220	913	3058
C_{max} (ng/mL)	503	387	2015	3792	391	199
$t_{1/2}$ (h)	8.3	5.9	5.9	6.2	7.7	7.0
V_{ss}	7.46	-	-	-	18.5	-
Kp, uu (@t_{max})	-	-	-	-	-	0.001

Figure 8. *In vivo* pharmacokinetic profile of **19** in male CD-1 mice (25-40 g) and male Crl:CD Sprague Dawley rats (250-400 g) dosed in 10% DMSO/90% hydroxypropyl-beta-cyclodextrin (20% w/v), n=3 per group. Free cell IC_{50} calculated by dividing measured cellular IC_{50} by free fraction in mouse plasma.

Initial evaluation of the *in vivo* efficacy of these inhibitors was conducted in mice with diet-induced obesity (DIO mice), which demonstrate impaired glucose control mediated by reduced sensitivity to insulin. Compound **18** was selected for these studies due to its high kinome selectivity, with sampling revealing slightly higher exposure in DIO mice relative to earlier pharmacokinetic studies (Figure 5) and no significant changes in exposure on repeat dosing for 14 days at 25 mg/kg. DIO mice treated with a single dose of 25 or 50 mg/kg **18** (in 1:9 DMSO:20% aqueous 2-hydroxypropyl-β-cyclodextrin) 4 hours prior to an oral glucose tolerance test (OGTT) show improved glucose control and increased insulin sensitivity relative to vehicle controls (figure 9A), with no significant difference in effect between the 25mg/kg and 50 mg/kg dose groups. Repeat administration of **18** twice daily for 14 days (in 1:9 DMSO:20% aqueous 2-hydroxypropyl-β-cyclodextrin on days 1-6, and 1% methyl cellulose on days 7-14) resulted in reduced baseline glucose and insulin levels, as well as reduced peak glucose levels following OGTT. While there was no effect on glucose AUCB2 in this experiment, the improvement in apparent insulin sensitivity was maintained and the overall profile was similar to the positive control liraglutide, which demonstrated a similar profile to that expected based on previous data. Unfortunately repeat dosing of 50 mg/kg **18** was not tolerated due to bloating of the gastrointestinal tract, (resulting in change of vehicle in the 25 mg/kg group at day 7) however this was not observed in subsequent tolerability studies with other compounds at significantly higher exposure/free cover. For example **19** has been dosed at 40 mg/kg uid (in 50:45:5 PEG400:water:ethanol) for 21 days in NGS mice with no observable adverse effects, suggesting the GI effects seen with **18** are unlikely to be target related.

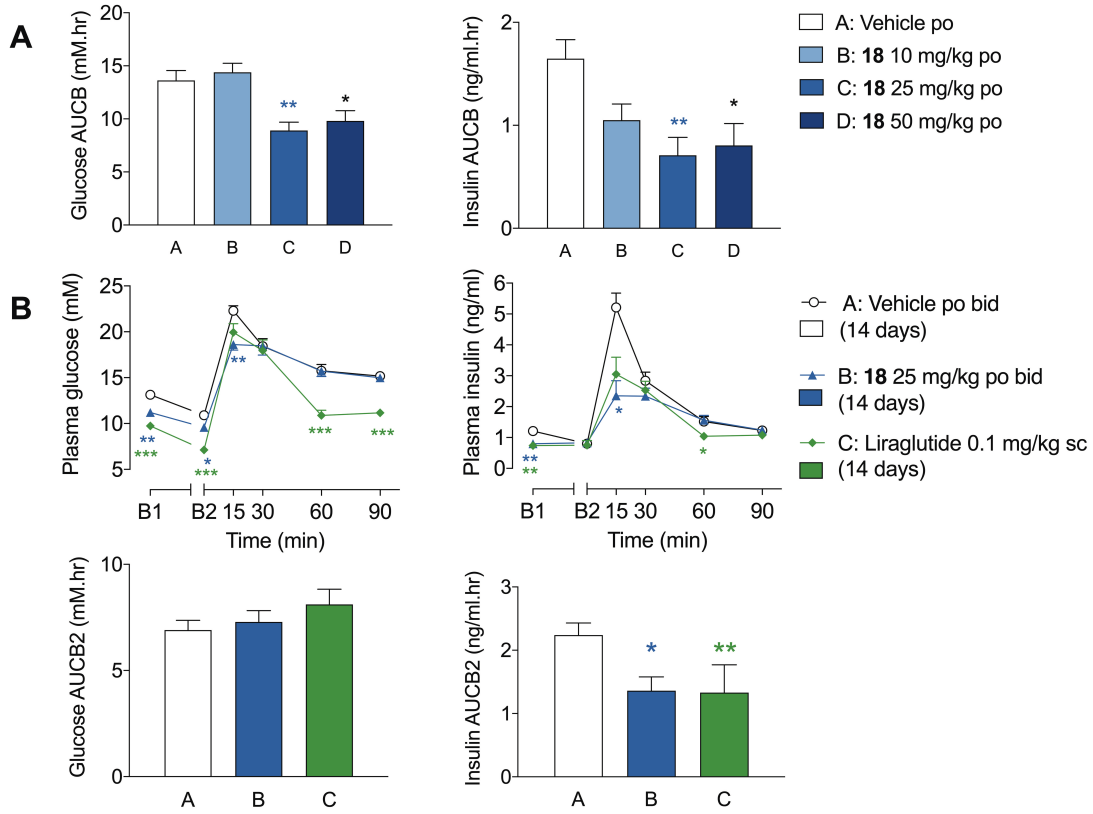

Figure 9. *In vivo* activity of compound **18** following oral glucose tolerance test (OGTT) in diet induced obesity mouse model (male C57Bl/6J mice) following single dose 4 hours prior to OGTT (**A**, n=6 per group) and 14 day repeat dosing (**B**, n=8 per group). Significant differences (from vehicle), determined by multiple t-test comparisons, are denoted by *p<0.05, **p<0.01 and ***p<0.001.

CHEMISTRY

Compounds **1** and **2** are known compounds and were prepared using the previously reported synthesis.[16] Analogues **3-8** were prepared from ethyl 2,4-dichloropyrimidine-5-carboxylate **20** *via* the 2-HOBt pyrimidine intermediate **21**, which was prepared as previously described,[16] by displacement of the 2-HOBt by the appropriate Boc-protected amine and Boc removal under acidic conditions (scheme 1).

Scheme 1. Synthetic route to compounds 3-8

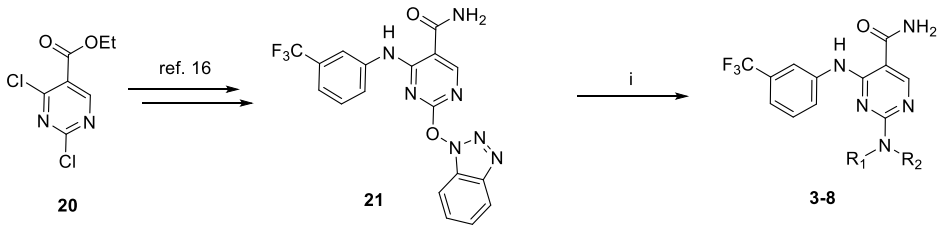

Reagents and conditions: (i) *N*-Boc-diamine, THF/DMF, RT, 30 mins; then DCM, 4 N HCl in dioxane, RT, 1 h, 81%.

To explore the aniline component, the tail was fixed to the (*S*)-3-aminopiperidine and a new synthetic strategy was sought to provide more rapid access to analogues with varied aniline substituents. The commercially available 2,4-dichloropyrimidine-5-carboxamide **22** allows formation of the final products in a typically 3-step process, by sequential displacement using the aniline followed by protected (*S*)-3-aminopiperidine and final acidic deprotection (scheme 2). The synthesis can be abbreviated by utilising excess unprotected (*S*)-3-aminopiperidine directly in the second stage, with the increased nucleophilicity of the cyclic secondary amine resulting in <1% formation of the product resulting from reaction at the primary amine. In general this approach complicates the purification of the final compounds and as such has not been extensively used, however may be useful when introducing acid-sensitive anilines.

Scheme 2. General synthetic route to compounds 9-19

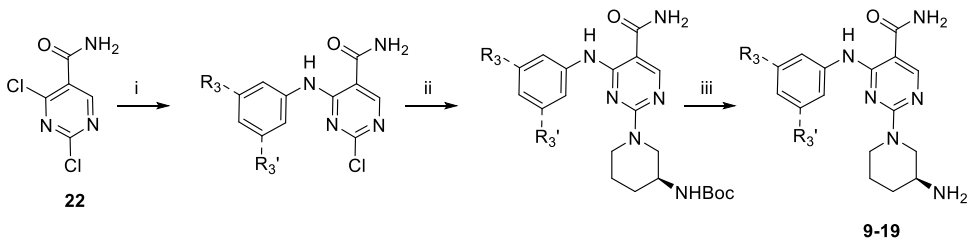

Reagents and conditions: (i) aniline, iPr_2NEt, MeCN or dioxane, reflux, 16 h; (ii) (*S*)-*tert*-butyl piperidin-3-ylcarbamate, DIPEA, solvent, RT, 2-16 h; (iii) TFA/DCM or 4 N HCl in dioxane, RT, 1 h, 10-73% over 3 steps.

The route outlined in scheme 2 provided ready access to compounds **9-14** by utilising commercially available anilines in stage 1. Subsequent synthetic effort focussed on preparation of anilines designed to develop the emerging SAR in this series. The symmetrical anilines **27** and **28** were initially synthesised by Suzuki reaction on dibromo precursors **23** and **24**, however it was later found that use of the nitro derivatives **25** and **26** results in a slightly cleaner reaction and easier purification, without adding extra steps as the nitro group and carbon-carbon double bonds are reduced in a single stage by heterogeneous hydrogenation.

Scheme 3. Synthesis of di-alkyl (hetero)anilines 27 and 28, used in compounds 15 and 19.

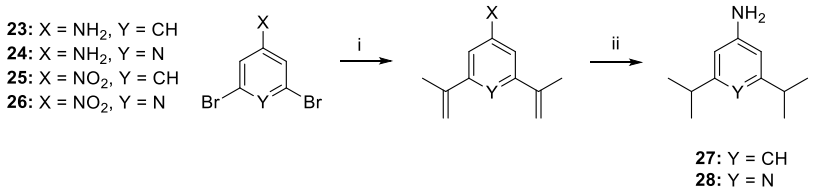

Reagents and conditions: (i) (4,4,5,5-tetramethyl-1,3,2-dioxaborolan-2-yl)isoprene, $NaHCO_3$, $PdCl_2dppf$ or $Pd(PPh_3)_4$, 1,4-dioxane, water, 90 °C, 4-16 h, 54-83%; (ii) H_2, Pd/C, MeOH, RT, 2-16 h, 75-98%.

In order to prepare the mixed ^{t}Bu/methylsulfone aniline **34** the commercially available nitro compound **29** was treated with chlorosulfonic acid in chloroform at reflux to afford the sulfonyl chloride **30**, which was reduced to the thiol **31** with triphenyl phosphine in refluxing toluene. Alkylation of **31** with methyl iodide provided the methyl sulfide **32**, which was oxidized with *m*-CPBA to the corresponding sulfone **33**, before nitro group reduction by heterogeneous hydrogenation to provide aniline **34**.

Scheme 4. Synthesis of aniline 34, used in compound 16

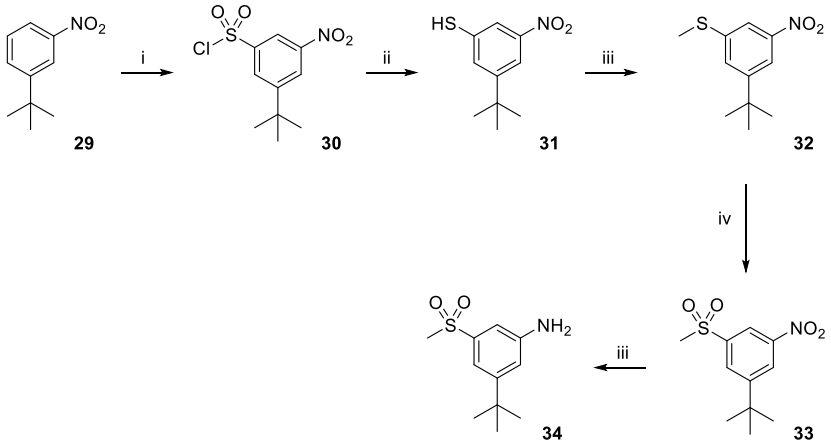

Reagents and conditions: (i) chlorosulfonic acid, $CHCl_3$, reflux, 48 h, 85%; (ii) $P(Ph)_3$, toluene, RT, 10 min, 72%; (iii) NaOH, MeI, EtOH, RT, 16 h, 98%; (iv) *m*-CPBA, DCM, 0 °C to RT, 2 h, 73%; (v) H_2 (5 atm.), Pd/C, MeOH, 16 h, 76%.

The cyanoisopropyl anilines used in compounds **17** and **18** were prepared from 3,5-dibromoaniline **27** by bis-benzylation to give **35** followed by treatment with

potassium 2-cyano-2-mehtylpropanoate and palladium catalyst[21] to afford a separable mixture of the symmetrical aniline **36** and partially reacted bromo derivative **37**. Compound **37** was submitted to a second Suzuki coupling to afford intermediate **38**. De-benzylation of **36** and **39** by heterogeneous hydrogenation provided the anilines **38** and **40**.

Scheme 6. Synthesis of 2-cyanoisopropyl substituted anilines used in compounds 17 and 18

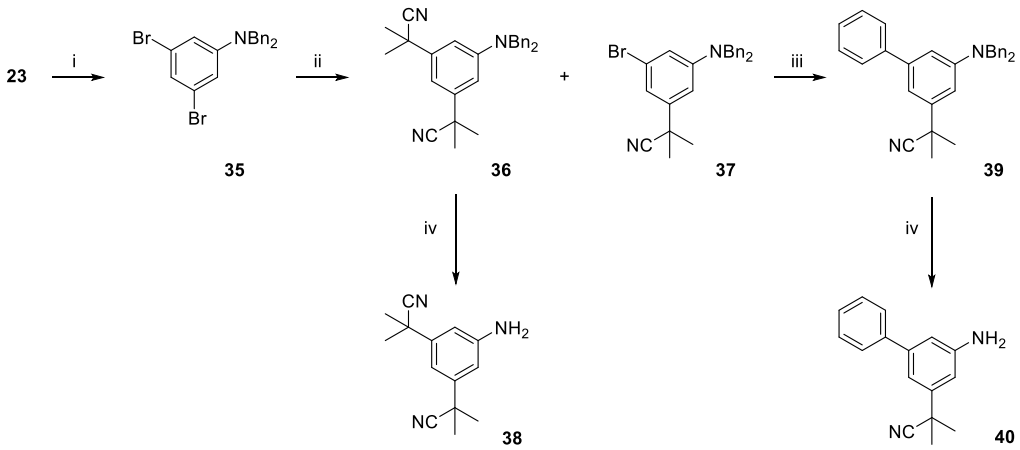

Reagents and conditions: (i) Benzyl bromide, K_2CO_3, MeCN, reflux, 24 h, 73%; (ii) potassium 2-cyano-2-methylpropanoate, mesitylene, Xantphos, $Pd_2allyl_2Cl_2$, 140 °C, 24 h, **36** = 53%, **37** = 20%; (iii) 4,4,5,5-tetramethyl-2-phenyl-1,3,2-dioxaborolane, $Pd(PPh_3)_2Cl_2$, K_2CO_3, dioxane:water, 100 °C, 1 h, 74%; (iv) H_2, Pd/C, MeOH:DCM, 18 h, 88-98%.

EXPERIMENTAL

***T_m*-Shift assays.** Thermal melting experiments were carried out using a Stratagene Mx3005p Real Time PCR machine (Agilent Technologies). Proteins were buffered in 10 mM HEPES, pH 7.5, 500 mM NaCl and assayed in a 96-well plate at a final concentration of 2 μM in a 20-μl volume. Compounds were added at a final

concentration of 10 μM (final DMSO concentration was 0.025%). SYPRO Orange (Molecular Probes) was added as a fluorescence probe at a dilution of 1:1,000 (v/v). Excitation and emission filters for the SYPRO-Orange dye were set to 465 nm and 590 nm, respectively. The temperature was raised with a step of 3 °C per minute from 25 °C to 96 °C, and fluorescence readings were taken at each interval. Experiments were performed in triplicate and the observed temperature shifts, ΔTm^{obs}, were recorded as the difference between the transition midpoints of sample and reference wells containing protein without ligand in the same plate and determined by non-linear least squares fit, reported in °C as the mean of the values obtained from 3 independent repeats.

CaMK1D ADP GLO Assay. Test compounds were prepared in 100% DMSO and 12 nL was dispensed to individual wells of a multiwell plate (Perkin Elmer, catalog no. 6007290). A reaction mixture containing full length His tagged CaMK1D (Fisher Scientific, PR6770A), calmodulin (Merck, 208694) and autocamtide-2 (SignalChem, A15-58) was prepared in assay buffer composed of 50 mM Tris-HCl pH 7.5, 10 mM MgCl2, 0.1 CaCl2 and 2 mM DTT. 7.88 μL of reaction mixture was added to each well to give a final assay concentration: 3 nM CaMK1D, 1 μM Calmodulin, 125 μM Autocamtide-2. Plates were centrifuged at 300 rpm for 30 s and incubated for 15 mins at 25°C. The enzyme reaction was initiated by the 4 μL addition of 30 μM ATP solution to give a final assay concentration 10 μM. Plates were centrifuged at 300 rpm for 30 s and then incubated at 25°C for 2 h. ADP-Glo (Promega, catalog no. V9102) was prepared according to manufacturer's instructions and equilibrated to room temperature, shielded from light. A 12 μL addition of ADP-Glo reagent was made to terminate the kinase reaction and deplete residual ATP. Plates were

centrifuged at 300 rpm for 30 s and then incubated at 25°C for 1 h. Following ATP depletion, 24 μL of ADP-Glo substrate was added to convert ADP to ATP and initiate a luciferase/luciferin chemiluminescent reaction. Plates were centrifuged at 300 rpm for 30 s and then incubated at 25°C for 30 min, shielded from light. After 30 minutes plates read with the EnVision® Multilabel Plate Reader, using Luminescence 700. Compound IC_{50} was determined using a 4-parameter equation, and reported as the geometric mean of the IC_{50} values obtained from 3 independent repeats.

pCaMK1D cell assay. MDA-MB-231 cells were purchased from the ATCC and routinely cultured in DMEM containing 10% FCS, 5U/mL penicillin/streptomycin (Gibco). MDA-MB-231-HA-CaMK1D cells were established by infecting MDA-MB-231 cells with modified pLVx-HA-CaMK1D lentivirus. Transduced cells were selected in media containing puromycin (2 μg/mL) and expression of CamK1D was verified by Western blotting using Rabbit anti-CamK1D mAb ([EPR3536(2)] (ab172618), used at 0.1 mg/mL). Custom made anti-pCamK1D (Ser179,Thr180) polyclonal antibodies were prepared by LifeTein (Hillsborough, NJ, USA), immunising MEGKGDVM(pS)(pT)ACGTPGYVA peptide and verified in a series of western blotting experiments. MDA-MB-231-HA-CaMK1D cells were cultured in DMEM Glutmax (31966-021, ThermoFisher) containing 10% fetal bovine serum (FBS) and 1 % penicillin-streptomycin. For the assay cells were seeded at 1.25 $x10^5$ cells/mL in 6-well plates and maintained at 37 °C in a humidified incubator with 5% CO_2 and 95% air for 48 hours. Then, cells were treated with compound for 4 h with a final DMSO concentration of 0.1 %, for each compound an 11-point serial dilution was used and DMSO included as a control. Media was aspirated and the cells washed with PBS. Cells were lysed, supernatants were recovered by centrifugation at 13 000

rpm, protein concentrations were measured, and equal amounts of total protein were separated by SDS-PAGE. Proteins were transferred to PVDF membranes (Bio-Rad), which was followed by blocking for 1 h in 5% milk in TBS-T. Membranes were incubated overnight at 4 °C with primary antibody: anti-pCamK1D (Ser179,Thr180) (1:1000) or total CaMK1D (1:10,000, ab172618, Abcam). Membranes were incubated with the corresponding HRP-conjugated secondary antibody (7074S, CST) for 1 h. Specific bands were detected using the enhanced-chemiluminescence reagent (Clarity Western substrate, Bio-Rad) and the ChemiDoc MP Gel Imaging System (Bio-Rad), and % change in pCAMK1D from control calculated using a ratio of pCaMK1D to total CaMK1D bands. Compound IC_{50} was determined using a 4-parameter equation, and reported as the geometric mean of the IC_{50} values obtained from 3 independent repeats.

Oral glucose tolerance test after acute and chronic/sub-acute (14 day) dosing. Male C57Bl/6J mice obtained from Charles River UK (Margate, Kent UK) at 7-8 weeks of age were group housed for 16 weeks (n = 3 in each cage) on a normal light/dark cycle (lights on: 07:00 – 19:00 h) with *ad libitum* access to a high fat diet (D12451 diet, 45% kcal as fat, 35% as carbohydrate; Research Diets, New Jersey, USA) and filtered water. **Acute dosing study.** Animals were allocated to dosing groups (6 mice per group) such that groups were balanced as closely as possible for mean body weight. The day prior to the OGTT, all animals were deprived of food (but not water) beginning approximately 16.45. The following morning the mice were dosed with vehicle or either 10 mg/kg, 25 mg/kg or 50 mg/kg **18** formulated in a vehicle of DMSO (10% final volume) and 20% (2-Hydroxypropyl)-β-cyclodextrin (90% final volume) by the oral route (beginning at 08.45). Four hours after dosing, a blood

sample was taken (B1) and 3 minutes later glucose administered (2 g/kg orally). Further blood samples were taken 10, 30, 60 and 90 minutes post glucose administration. Between blood sampling, animals were returned to the home cage with free access to water (but not food). Blood samples (approx. 30 µl) were collected into lithium heparinised tubes (Sarstedt Microvette CB300LH) and plasma separated by centrifugation to produce a single aliquot of plasma which was frozen (approx. -80°C) and subsequently assayed for glucose (in duplicate; Thermoelectron Infinity glucose reagent TR15498) and insulin (single replicate; Alpco mouse ultrasensitive insulin kit 80 -INSMSU-E10). **Chronic dosing study.** Upon completion of the OGTT, all animals were singly housed with food provided as above for two weeks prior to the onset of the baseline phase of the chronic study. Upon single housing after the OGTT, mice were placed on a reverse-phase light dark cycle (lights off: 09:30 – 17:30). Following this period the animals underwent a 5-day baseline phase where they were be dosed twice daily with vehicle at approximately 08:45 and 16:45 each day. Towards the end of the baseline phase mice were reallocated to dosing groups (8 animals per group) such that groups within the study were balanced as closely as possible for body weight and food and water intake and previous treatment. From Day 1 onwards, mice were dosed orally twice daily with 25 mg/kg **18** formulated in a vehicle of DMSO (10% final volume) and 20% (2-Hydroxypropyl)-β-cyclodextrin (90% final volume) on days 1-6 and 1% methyl cellulose at 5 mL/kg on subsequent days, or twice daily orally with vehicle alone, or with subcutaneous dosing of 0.1 mg/kg liraglutide (Bachem) formulated in pH 7.4 phosphate buffer solution. Oral dosing began at approximately 08:45 and 16.45, with subcutaneous dosing at 08:45 only. Dosing continued until the morning of Day 14, when food was removed beginning at approximately 16:45. Approximately 16h post-fast the animals were be moved to a

separate room maintained under normal lighting and dosed with vehicle or test compounds in the normal manner to a timed schedule 4 hours prior to the administration of the glucose challenge (2.0 g/kg po). Blood samples were taken immediately prior to dosing (B1), immediately prior to glucose administration (B2) and 15, 30, 60 and 90 minutes after glucose administration. All blood samples (approx. 30 µl) were taken in lithium heparin-coated tubes (Sarstedt CB300LH) and spun as soon as possible in a centrifuge. Plasma samples were stored frozen (approx. -80ºC) until determination of plasma glucose (in duplicate; Thermoelectron Infinity glucose reagent TR15498) and insulin (single replicate; Alpco mouse ultrasensitive insulin kit 80 -INSMSU-E10). Plasma glucose and insulin data from the OGTTs were analysed by robust regression with treatment as a factor and bleeding order and Day 1 body weight as covariates. AUCs for 0 to 60 (following single dose) and 0 to 90 minutes (following repeat dose) were calculated (as total AUC and AUC from baseline) by trapezoidal rule and analysed by the same methodology. In all cases, this analysis was followed by multiple t-test comparisons to determine significant differences in both absolute levels and AUC from the vehicle group.

General chemistry experimental. Commercially available and enantiomerically pure *tert*-butyl (*S*)-piperidin-3-ylcarbamate and *tert*-butyl (*R*)-piperidin-3-ylcarbamate were purchased from Carbosynth Ltd. (e.g. FB11271) and used as provided. All other commercially available starting materials, reagents and solvents were purchased and used without further purification. The reactions were monitored by thin-layer chromatography (60 on aluminium sheets with F254) or by LCMS. LC data was obtained using a Waters ACQUITY UPLC PDA detector scanning between 210-400 nm. Mass spectrometry data was acquired using a Waters ACQUITY QDa

detector scanning in the positive (ES^+) and negative (ES^-) modes between *m/z* 100-1000. Separation of components was achieved using a Waters ACQUITY UPLC BEH C18 1.7 μm 2.1 × 50 mm column coupled to a Waters ACQUTY UPLC BEH C18 1.7 μm VanGuard pre-column 2.1 × 5 mm. Columns were maintained at 40 °C throughout acquisition. Data was processed using MassLynx V4.1. Values of purity were obtained through analysis of the peak areas in the LC trace between 0.40 min. and 3.50 min. Purity and identity of all tested compounds were established by a combination of mass spectrometry, HRMS and NMR spectra as described below. Purification of isolated products was carried out by column chromatography in silica gel (particle size 40-63 microns, Merk) or medium pressure liquid chromatography (MPLC) on a CombiFlash Companion (Teledyne ISCO) with AquGold pre-packed reverse-phase C18 columns. Nuclear magnetic resonance (NMR) spectra were obtained either on a Bruker Advance 400 or 500 MHz spectrometer. Chemical shifts (δ) are reported in ppm using the residual signal of the deuterated solvent (MeOD-*d4*, $CDCl_3$, DMSO-*d6*) as internal standard, and coupling constants (*J*) are reported in Hertz (Hz). The multiplicities are abbreviated as follows: s = singlet, d = doublet, t = triplet, q = quartet, quint = quintet, sext = sextet, sept = septet, m = multiplet, br = broad signal. High-resolution mass spectra were obtained on a Thermo Finigan MAT95XP, magnetic sector mass spectrometer, electron ionisation. HPLC Method 1: Performed on a Shimadzu UFLCXR system coupled to an Applied Biosystems API2000. Column maintained at 40 ^oC. Column: Phenomenex Gemini-NX 3 μm-110 Å C18, 50x2 mm. Total flow rate 0.5 mL/min. UV detection at 220 nm (channel 2) and 254 nm (channel 1). Gradient: Pre-equilibration run for one min at 5% B; then method run: 5 to 98% solvent B in 2 min, 98% B for 2 min, 98 to 5% B in 0.5 min then 5% for one min. Acid method: Solvent A = 0.1% Formic Acid in water; solvent

B = 0.1% Formic Acid in MeCN. HPLC Method 2: Performed on an Agilent HPLC. Column: Waters X-Select C18 2.5 μm, 4.6x30 mm, using standard acidic (0.1% Formic acid) 4 min method, 5-95% MeCN/water, UV detection at 254 nm). HPLC Method 3: Performed on a Waters ACQUITY UPLC with PDA detector scanning between 210-400 nm. Mass spectral data was obtained using a Waters ACQUITY QDa detector scanning in the positive (ES+) and negative (ES-) modes between m/z 100-650. Samples were passed through a Waters ACQUITY UPLC BEH C18 1.7 μm 2.1 x 50 mm column coupled to a Waters ACQUITY UPLC BEH C18 VanGuard precolumn 2.1 x 5 mm. Gradient: Pre-equilibration run for 30 s at 5% B; then method run: 5 to 95% solvent B in 2 min, 95% B for 30 s, 95 to 5% B in 6 s then 5% B for 54 s. The column was maintained at 40 °C. Acid method: Solvent A = 0.1% Formic Acid in water; solvent B = MeCN. Base method: Solvent A = 0.1% ammonium hydroxide in water; solvent B = MeCN. HPLC Method 4: Performed on an Agilent HPLC. Column: Waters X-Bridge C18 2.5 μm, 4.6x30 mm, using standard basic (0.1% ammonium bicarbonate) 4 min method, 5-95% MeCN/water, UV detection at 254 nm). Compound purity was assessed by HPLC method 1 using both Phenomenex Gemini-NX 3 μm- 110 Å C18, 50x2 mm and Phenomenex Luna-NX 3 μm- 110 Å PFP, 50x2 mm columns, with uv detection at 254 nm. All compounds demonstrate purity >95% by both methods, with the exception of **5** which demonstrates 92.5% purity on the Gemini C-18 column and 96.4% purity on the Luna PFP column.

2-((2-aminoethyl)amino)-4-((3-(trifluoromethyl)phenyl)amino)pyrimidine-5-carboxamide hydrochloride (1). Compound prepared following a reported method.[16] **^{1}H-NMR** (400 MHz, DMSO-d_6) δ 12.34 (s, 1H), 8.91 (s, 1H), 8.61 (br s, 2H), 8.32 (br s, 3H), 8.13 (s, 1H), 7.90 (d, J = 8.1 Hz, 1H), 7.70 (app. t, J = 8.1 Hz, 1H), 7.55 (d, J = 8.1 Hz, 1H), 3.64 (app. q, J = 5.6 Hz, 2H), 3.01 (app. q, J = 5.6 Hz, 2H); **LC-MS**

m/z (ES^+) $(M+H)^+$ 341.2; t_R = 1.98 min. HPLC Method 1. **HRMS** (ES-TOF): *m/z* calcd. for $C_{14}H_{16}F_3N_6O$: 341.1332, found 341.1346 $[M+H]^+$.

2-((2-aminoethyl)amino)-*N*-methyl-4-((3-(trifluoromethyl)phenyl)amino)pyrimidine-5-carboxamide (2). Compound prepared following a reported method.[16] **^{1}H-NMR** (DMSO-d_6) δ 12.21 (s, 1H), 9.30 (d, *J* = 3.9 Hz, 1H), 8.88 (s, 1H), 8.66 (app. t, *J* = 5.2 Hz, 1H), 8.26 (br s, 3H), 8.14 (s, 1H), 7.91 (d, *J* = 7.9 Hz, 1H), 7.70 (app. t, *J* = 7.9 Hz, 1H), 7.56 (d, *J* = 7.8 Hz, 1H), 3.64 (app. q, *J* = 4.8 Hz, 2H), 3.02 (app. q, *J* = 4.8 Hz, 2H), 2.78 (d, *J* = 4.4 Hz, 3H); **LC-MS** *m/z* (ES^+) $(M+H)^+$ 355.2.; t_R = 1.99 min. HPLC Method 1. **HRMS** (ES-TOF): *m/z* calcd. for $C_{15}H_{17}F_3N_6ONa$: 377.1308, found 377.1301 $[M+Na]^+$.

2-((2-aminoethyl)(methyl)amino)-4-((3-(trifluoromethyl)phenyl)amino)pyrimidine-5-carboxamide hydrochloride (3). To a suspension of 2-((1H-benzo[d][1,2,3]triazol-1-yl)oxy)-4-((3-(trifluoromethyl)phenyl)amino)pyrimidine-5-carboxamide **21**, prepared following a reported method[16] (0.11 g, 0.25 mmol) in THF (2 mL) and DMF (1 mL) was added *N*-boc-2-methylamino-ethylamine (50 mg , 0.28 mmol) and stirred for 30 min at room temperature. The mixture was diluted with water and extracted with AcOEt. The organic layer was dried over anhydrous Na_2SO_4, and concentrated under reduced pressure. ***m/z*** (ES^+) $(M+H)^+$ 455.0; t_R = 2.74 min. HPLC Method 1. The crude was dissolved in CH_2Cl_2 (2 mL) and 4N HCl in dioxane (5 mL) was added. The suspension was stirred at RT for 1 h (completion monitored by HPLC). The suspension was concentrated and Et_2O was added to induce precipitation. The resulting white solid was centrifuged, washed again with Et_2O and dried under

vacuum affording the titled compound (50 mg, 81%). **^{1}H-NMR** (400 MHz, MeOD-d_4) δ 8.61 (s, 1H), 8.09 (br s, 1H), 7.78 (d, J = 7.6 Hz, 1H), 7.66 (app. t, J = 7.8 Hz, 1H), 7.57 (d, J = 7.6 Hz, 1H), 3.99 (t, J = 5.7 Hz, 2H), 3.36 (s, 3H), 3.26 (br s, 2H); **LC-MS** *m/z* (ES^+) $(M+H)^+$ 355.2; t_R = 2.09 min. HPLC Method 1. **HRMS** (ES-TOF): *m/z* calcd. for $C_{15}H_{18}F_3N_6O$: 355.1489, found 355.1503 $[M+H]^+$.

2-(methyl(2-(methylamino)ethyl)amino)-4-((3-(trifluoromethyl)phenyl)amino)pyrimidine-5-carboxamide hydrochloride (4). Prepared in analogous manner to **3** using *N*-boc-2,4-dimethylamino-ethylamine. **^{1}H-NMR** (400 MHz, MeOD-d_4) δ 8.62 (s, 1H), 8.06 (br s, 1H), 7.82 (d, J = 7.8 Hz, 1H), 7.69 (app. t, J = 7.8 Hz, 1H), 7.60 (br d, J = 7.1 Hz, 1H), 4.05 (t, J = 5.6 Hz, 2H), 3.38 (s, 3H), 3.32 (br s, 2H), 2.59 (br s, 3H); **LC-MS** *m/z* (ES^+) $(M+H)^+$ 369.2; t_R = 2.12 min. HPLC Method 1. **HRMS** (ES-TOF): *m/z* calcd. for $C_{16}H_{20}F_3N_6O$: 369.1645, found 369.1659 $[M+H]^+$.

2-((2-(dimethylamino)ethyl)(methyl)amino)-4-((3-(trifluoromethyl)phenyl)amino)pyrimidine-5-carboxamide hydrochloride (5). Prepared in analogous manner to **3** *N*-boc-2,4,4-trimethylamino-ethylamine. **^{1}H-NMR** (400 MHz, MeOD-d_4) δ 8.61 (s, 1H), 7.96 (br s, 1H), 7.82 (d, J = 7.1 Hz, 1H), 7.70 (app. t, J = 7.4 Hz, 1H), 7.63 (br s, 1H), 4.09 (app. t, J = 5.4 Hz, 2H), 3.42 (br s, 2H), 3.33 (s, 3H), 2.68 (br s, 6H); **LC-MS** *m/z* (ES^+) $(M+H)^+$ 383.2; t_R = 2.12 min. HPLC Method 1. **HRMS** (ES-TOF): *m/z* calcd. for $C_{17}H_{22}F_3N_6O$: 383.1802, found 383.1824 $[M+H]^+$.

(*rac*)-2-(3-aminopiperidin-1-yl)-4-((3-(trifluoromethyl)phenyl)amino)pyrimidine-5-carboxamide hydrochloride (6). Prepared in analogous manner to **3** using (±)*tert*-butyl-piperidin-3-ylcarbamate. **^{1}H-NMR** (400 MHz, MeOD-d_4) δ 8.60 (s, 1H), 8.10 (br s, 1H), 7.81 (br d, J = 7.1 Hz, 1H), 7.67 (t, J = 7.8 Hz, 1H), 7.56 (d, J = 7.8 Hz, 1H), 4.35 (dd, J =13.5, 3.7 Hz, 1H), 4.06 (br s, 1H), 3.73 (dd, J = 13.5, 8.4 Hz, 1H), 3.64-3.57 (m, 1H), 3.54-3.48 (m, 1H), 2.24-2.16 (m, 1H), 2.02-1.94 (m, 1H), 1.88-1.75 (m, 2H); **LC-MS** *m/z* (ES^+) $(M+H)^+$ 381.4; t_R = 2.14 min. HPLC Method 1. **HRMS** (ES-TOF): *m/z* calcd. for $C_{17}H_{20}F_3N_6O$: 381.1645, found 381.1662 $[M+H]^+$.

(*R*)-2-(3-aminopiperidin-1-yl)-4- ((3-(trifluoromethyl) phenyl) amino) pyrimidine-5-carboxamide hydrochloride (7). Prepared in analogous manner to **3** using *tert*-butyl (*R*)-piperidin-3-ylcarbamate. **^{1}H-NMR** (400 MHz, MeOD-d_4) δ 8.60 (s, 1H), 8.10 (br s, 1H), 7.81 (br d, J = 7.1 Hz, 1H), 7.67 (t, J = 7.8 Hz, 1H), 7.56 (d, J = 7.8 Hz, 1H), 4.35 (dd, J =13.5, 3.7 Hz, 1H), 4.06 (br s, 1H), 3.73 (dd, J = 13.5, 8.4 Hz, 1H), 3.64-3.57 (m, 1H), 3.54-3.48 (m, 1H), 2.24-2.16 (m, 1H), 2.02-1.94 (m, 1H), 1.88-1.75 (m, 2H); **LC-MS** *m/z* (ES^+) $(M+H)^+$ 381.4; t_R = 2.14 min. HPLC Method 1. **HRMS** (ES-TOF): *m/z* calcd. for $C_{17}H_{20}F_3N_6O$: 381.1645, found 381.1655 $[M+H]^+$.

(*S*)-2-(3-aminopiperidin-1-yl)-4- ((3-(trifluoromethyl) phenyl) amino) pyrimidine-5-carboxamide hydrochloride (8). Prepared in analogous manner to **3** using *tert*-butyl (*S*)-piperidin-3-ylcarbamate. **^{1}H-NMR** (400 MHz, MeOD-d_4) δ 8.60 (s, 1H), 8.10 (br s, 1H), 7.81 (br d, J = 7.1 Hz, 1H), 7.67 (t, J = 7.8 Hz, 1H), 7.56 (d, J = 7.8 Hz, 1H), 4.35 (dd, J =13.5, 3.7 Hz, 1H), 4.06 (br s, 1H), 3.73 (dd, J = 13.5, 8.4 Hz, 1H), 3.64-3.57 (m, 1H), 3.54-3.48 (m, 1H), 2.24-2.16 (m, 1H), 2.02-1.94 (m, 1H),

1.88-1.75 (m, 2H); **LC-MS** *m/z* (ES^+) $(M+H)^+$ 381.0; t_R = 2.15 min. HPLC Method 1. **HRMS** (ES-TOF): *m/z* calcd. for $C_{17}H_{20}F_3N_6O$: 381.1645, found 381.1655 $[M+H]^+$.

(*S*)-2-(3-aminopiperidin-1-yl)-4- ((4-(trifluoromethyl) phenyl) amino) pyrimidine-5-carboxamide hydrochloride (9)

3,5-bis(trifluoromethyl)aniline (85 mg, 0.37 mmol) was added to a solution of 2,4-dichloropyrimidine-5-carboxamide **22** (75 mg, 0.39 mmol) and DIPEA (0.17 mL, 0.98 mmol) in dioxane (5 mL) and stirred at 80°C for 16 h. The reaction was concentrated under reduced pressure. (38 mg, 20%). **LC-MS** *m/z* (ES^+) $(M+H)^+$ 385.0; t_R = 2.44 min. HPLC Method 2.

(*S*)-tert-butyl piperidin-3-ylcarbamate (62 mg, 0.23 mmol) was added to a solution of 4-((3,5-bis(trifluoromethyl)phenyl)amino)-2-chloropyrimidine-5-carboxamide (38 mg, 0.10 mmol) and TEA (69 µL, 0.49 mmol) in dioxane (10 mL). The reaction was stirred at RT for 16 h. The mixture was diluted with Et_2O (10 mL), filtered and washed with CH_2Cl_2/ MeOH/ Et_2O (9:1:9 mL). No further purification was required. (20 mg, 19% yield). **LC-MS** *m/z* (ES^+) $(M+H)^+$ 549.0; t_R = 2.75 min. HPLC Method 2.

(*S*)-*tert*-butyl (1-(4-((3,5-bis(trifluoromethyl)phenyl)amino)-5-carbamoylpyrimidin-2-yl)piperidin-3-yl)carbamate (20 mg, 0.04 mmol) was treated with TFA (0.10 mL, 1.08 mmol) in CH_2Cl_2 (1 mL). The reactions were strirred for 2 h and concentrated under reduced pressure. The residues were diluted in MeOH (0.20 mL) and loaded onto a SCX cartridge, washing with MeOH (3 column volumes) and eluting with 1% NH_3 MeOH (3 column volumes). The ammonical MeOH was removed under reduced pressure to give the product (12 mg, 16% yield over 3 steps). **^{1}H-NMR** (400 MHz, MeOD-d_4) δ 8.63 (s, 1H), 8.41-8.31 (m, 2H), 7.60 (s, 1H), 4.67-4.60 (m, 1H), 4.50-

4.43 (m, 1H), 3.24-3.18 (m, 1H), 3.03 (dd, *J* = 12.7, 9.4 Hz, 1H), 2.90-2.84 (m, 1H), 2.12-2.04 (m, 1H), 1.91-1.83 (m, 1H), 1.68-1.43 (m, 2H). **LC-MS** *m/z* (ES^+) $(M+H)^+$ 449.0; t_R = 1.59 min. HPLC Method 2; **HRMS** (ES-TOF): *m/z* calcd. for $C_{18}H_{19}F_6N_6O$: 449.1519, found 449.1538 $[M+H]^+$.

(*S*)-2-(3-aminopiperidin-1-yl)-4-((3-(*tert*-butyl)phenyl)amino)pyrimidine-5-carboxamide hydrochloride (10)

Prepared in analogous manner to **9** using 3-*tert*-butyl-aniline. Compound isolated as HCl salt. **^{1}H-NMR** (400 MHz, MeOD-d_4) δ 8.54 (s, 1H), 7.72 (s, 1H), 7.41 (d, *J* = 7.8 Hz, 1H), 7.28 (t, *J* = 7.9 Hz, 1H), 7.14 (dd, *J* = 7.8, 2.0 Hz, 1H), 4.62 (dd, *J* = 12.6, 3.9 Hz, 1H), 4.53 (d, *J* = 13.2 Hz, 1H), 3.18-3.12 (m, 1H), 2.96 (dd, *J* = 12.7, 9.4 Hz, 1H), 2.85-2.78 (m, 1H), 2.07-1.99 (m, 1H), 1.84-1.77 (m, 1H), 1.63-1.39 (m, 2H), 1.36 (s, 9H); **LC-MS** *m/z* (ES^+) $(M+H)^+$ 369; t_R = 2.01 min. HPLC Method 2. **HRMS** (ES-TOF): *m/z* calcd. for $C_{20}H_{29}N_6O$: 369.2397, found 369.2412 $[M+H]^+$.

(*S*)-2-(3-aminopiperidin-1-yl)-4-((3-(methylsulfonyl)phenyl)amino)pyrimidine-5-carboxamide (11).

Prepared in analogous manner to **9** using 3(methylsulfonyl-aniline. **^{1}H-NMR** (400 MHz, MeOD-d_4) δ 9.08 (s, 1H), 8.61 (s, 1H), 7.67-7.55 (m, 2H), 7.49 (s, 1H), 4.78 (s, 1H), 4.62 (s, 1H), 3.16-3.10 (m, 4H), 2.99-2.92 (m, 2H), 2.09 (br s, 1H), 1.89-1.86 (m, 1H), 1.65-1.59 (m, 1H), 1.53-1.44 (m, 1H); **LC-MS** *m/z* (ES^+) $(M+H)^+$ 391; t_R = 1.30 min. HPLC Method 2; **HRMS** (ES-TOF): *m/z* calcd. for $C_{17}H_{23}N_6O_3S$: 391.1547, found 391.1554 $[M+H]^+$.

(*S*)-4-([1,1'-biphenyl]-3-ylamino)-2-(3-aminopiperidin-1-yl)pyrimidine-5-carboxamide hydrochloride (12)

Prepared in analogous manner to **9** using 3-amino-1,1'-biphenyl. Compound isolated as HCl salt. **^{1}H-NMR** (400 MHz, MeOD-d_4) δ 8.55 (s, 1H), 7.83 (br s, 1H), 7.64-7.61 (m, 3H), 7.56-7.51 (m, 2H), 7.46 (t, J = 7.6 Hz, 2H), 7.39-7.35 (m, 1H), 4.34 (dd, J = 13.8, 3.5 Hz, 1H), 4.04 (br s, 1H), 3.78 – 3.70 (m, 1H), 3.63-3.54 (m, 1H), 3.54-3.47 (m, 2H), 2.23-2.16 (m, 1H), 1.99-1.89 (m, 1H), 1.89-1.73 (m, 2H). **LC-MS** *m/z* (ES^+) $(M+H)^+$ 389.1; t_R = 2.25 min. HPLC Method 1; **HRMS** (ES-TOF): *m/z* calcd. for $C_{22}H_{25}N_6O$: 389.2084, found 389.2101 $[M+H]^+$.

(*S*)-2-(3-aminopiperidin-1-yl)-4-((3-(2-cyanopropan-2-yl)phenyl)amino)pyrimidine-5-carboxamide (13)

Prepared in analogous manner to **9** using 2-(3-aminophenyl)-2-methylpropanenitrile. **^{1}H-NMR** (400 MHz, MeOD-d_4) 8.56 (s, 1H), 8.08 (app. t, J = 2.0 Hz, 1H), 7.47-7.36 (m, 2H), 7.21 (ddd, J = 7.4, 2.0, 1.3 Hz, 1H), 4.67-4.60 (m, 1H), 4.54 (d, J = 13.2 Hz, 1H), 3.19-3.09 (m, 1H), 2.96 (dd, J = 12.7, 9.4 Hz, 1H), 2.81-2.79 (m, 1H), 2.03 (br s, 1H), 1.84 (br s, 1H), 1.77 (s, 6H), 1.64-1.52 (m, 1H), 1.49-1.36 (m, 1H); **LC-MS** *m/z* (ES^+) $(M+H)^+$ 380.0; t_R = 1.66 min. HPLC Method 2; **HRMS** (ES-TOF): *m/z* calcd. for $C_{20}H_{25}N_7ONa$: 402.2013, found 402.2016 $[M+Na]^+$.

(*S*)-2-(3-aminopiperidin-1-yl)-4-((3,5-di-tert-butylphenyl)amino)pyrimidine-5-carboxamide (14)

Prepared in analogous manner to **9** using 3,5-di-*tert*-butyl-aniline. **^{1}H-NMR** (400 MHz, MeOD-d_4) δ 8.53 (s, 1H), 7.43 (d, J = 1.7 Hz, 2H), 7.38 (t, J = 1.7 Hz, 1H), 4.27 (dd, J = 13.6, 3.5 Hz, 1H), 4.11 (br s, 1H), 3.85-3.74 (m, 1H), 3.69-3.60 (m, 1H),

3.54-3.46 (m, 1H), 2.23-2.14 (m, 1H), 1.98-1.89 (m, 1H), 1.89-1.73 (m, 2H), 1.35 (s, 18H); **LC-MS** *m/z* (ES^+) $(M+H)^+$ 425.2; t_R = 2.43 min. HPLC Method 1. **HRMS** (ES-TOF): *m/z* calcd. for $C_{24}H_{37}N_6O$: 425.3023, found 425.3036 $[M+H]^+$.

(*S*)-2-(3-aminopiperidin-1-yl)-4-((3,5-diisopropylphenyl)amino)pyrimidine-5-carboxamide (15)

Step 1; 1-Nitro-3,5-di(prop-1-en-2-yl)benzene. A mixture of 1,3-dibromo-5-nitrobenzene (2.0 g, 7.14 mmol), 4,4,5,5-tetramethyl-2-(1-methylethenyl)-1,3,2-dioxaborolane (3.6 g, 21.42 mmol), $Pd(PPh_3)_4$, (164 mg, 0.142 mmol), and K_2CO_3 (3.0 g, 21.4 mmol) was heated at 100 ^oC in dioxane–H_2O (100 mL) with stirring under N_2. After cooling, the reaction was quenched with saturated aq. NH_4Cl solution, extracted with EtOAc, dried over Na_2SO_4, filtered, and evaporated. The residue was chromatographed on SiO_2 gel using CH_2Cl_2–hexane gradient elution to afford the pure title compound (1.20 g, 83%). **LC** t_R 3.22 min (> 95%; method 1).

Step 2; 3,5-Diisopropylaniline (27). The material from the previous step (1.2 g, 5.9 mmol) was dissolved in MeOH (20 mL). The solution was stirred, purged with N_2, and then treated with H_2 over Pd(C) overnight. The catalyst was removed by filtration and the solution was evaporated. The residue of title compound (1.02 g, 98%) was used in the next step without further purification. **LC-MS** *m/z* (ES^+) 177.7 $[M+H]^+$ t_R 2.47 min (Method 1).

Step 3; 2-chloro-4-((3,5-diisopropylphenyl)amino)pyrimidine-5-carboxamide. The material from the previous step (1.02 g, 5.75 mmol), 2,4-dichloropyrimidine-5-carboxamide (1.2 g, 6.2 mmol), and iPr_2NEt (1.3 mL) were dissolved in MeCN (20 mL) and the mixture was heated under reflux for 3 h. The resulting solution was evaporated, redissolved in the minimum volume of CH_2Cl_2 and chromatographed on

SiO_2 gel using CH_2Cl_2–EtOAc gradient elution. Fractions containing pure title product were pooled, evaporated, and triturated with Et_2O (1.34 g, 71%). **LC-MS** (ES^+) t_R 3.18 min (> 95%; method 1), *m*/*z* 332.8 $[M+H]^+$.

Step 4; *tert*-butyl (*S*)-(1-(5-carbamoyl-4-((3,5-diisopropylphenyl)amino)pyrimidin-2-yl)piperidin-3-yl)carbamate. The material from the previous step (66 mg, 0.20 mmol) was reacted with *tert*-butyl (*S*)-piperidin-3-ylcarbamate (44 mg, 0.22 mmol) and iPr_2NEt (0.1 mL) by stirring in MeCN (3 mL) at 50 ^oC for 20 h. After cooling, the reaction mixture was evaporated, diluted with H_2O, extracted with CH_2Cl_2, dried over Na_2SO_4, filtered, and evaporated. The residue was chromatographed on SiO_2 gel using CH_2Cl_2–EtOAc gradient elution to afford the pure title compound (74 mg, 75%). **LC-MS** (ES^+) t_R 3.08 min (91%; method 1), *m*/*z* 497.8 $[M+H]^+$.

Step 5; (*S*)-2-(3-aminopiperidin-1-yl)-4-((3,5-diisopropylphenyl)amino)pyrimidine-5-carboxamide (16)

The material from the previous step (74 mg, 0.149 mmol) was treated with excess HCl in dioxane at room temperature for 4 h to afford the title compound (55 mg, 92.6%) after evaporation and trituration with Et_2O. **^{1}H-NMR** (400 MHz, d_6-DMSO) δ: 8.67 (s, 1H), 7.25 (s, 2 H), 7.00 (s, 1 H), 4.16 (m, 1H), 3.03-3.25 (m, 3H), 2.88 (m, 3 H), 1.85-2.06 (m, 2H), 1.68 (m, 2 H), 1.18 (app. dd, J = 7.0 Hz, 1.2 Hz, 12 H); **LC-MS** (ES^+) t_R 2.36 min (87.2%; method 1), *m*/*z* 397.0 $[M+H]^+$; **HRMS** (ES-TOF): *m*/*z* calcd. for $C_{22}H_{33}N_6O$: 397.2710, found 397.2723 $[M+H]^+$.

(*S*)-2-(3-aminopiperidin-1-yl)-4-((3-(tert-butyl)-5-(methylsulfonyl)phenyl)amino) pyrimidine-5-carboxamide (16)

Step-1: 3-(*tert*-butyl)-5-nitrobenzenesulfonyl chloride (30). To a solution of 1-(*tert*-butyl)-3-nitrobenzene (179 mg, 1 mmol) in $CHCl_3$ (15 mL), chlorosulfonic acid (167 µL, 2.5 mmol) was added in one portion and the mixture stirred at reflux for 48 h. Upon complete consumption of the starting material, water (15 mL) and DCM (15 mL) were added, the crude was partitioned, the aqueous layer extracted with DCM (2 x 20 mL) and the combined organic layers washed with brine, dried with $MgSO_4$ and condensed. The crude was purified by flash column chromatography (gradient: hexane/ethyl acetate = (9:1) to (3:1)) to give the desired product as a brown oil (235 mg, 85%). **^{1}H NMR** (300 MHz, $CDCl_3$) δ 8.73 (t, *J* = 1.9 Hz, 1H), 8.62 (t, *J* = 1.9 Hz, 1H), 8.35 (t, *J* = 1.9 Hz, 1H), 1.48 (s, 9H); **MS** *m/z* (ES) $[M+Na]^+$ 300.0.

Step-2: 3-(*tert*-butyl)-5-nitrobenzenethiol (31): To a solution of 3-(*tert*-butyl)-5-nitrobenzenesulfonyl chloride (0.28 g, 1.0 mmol) in toluene (8 mL), triphenyl phosphine (0.79 mg, 3.0 mmol) was added portion wise and the reaction was stirred at room temperature for 10 min. Upon complete consumption of the starting material, water (4 mL) was added and the mixture was partitioned. The organic layer was extracted with aqueous NaOH (10 %, 2 × 15 mL) and the aqueous layer was washed AcOEt (2 × 15 mL), acidify with concentrated HCl and extracted with CH_2Cl_2 (2 × 15 mL). The combined organic layers were dried with $MgSO_4$ and condensed to give the desired product as a clear oil (0.15 g, 72%). **^{1}H-NMR** (400 MHz, $CDCl_3$) δ 7.94 (app. t, *J* = 1.9 Hz, 1H), 7.87 (app. t, *J* = 1.9 Hz, 1H), 7.49 (app. t, *J* = 1.9 Hz, 1H), 3.62 (s, 1H), 1.27 (s, 9H); **^{13}C-NMR** (101 MHz, $CDCl_3$) δ 177.5, 154.1, 133.1, 132.0, 121.0, 117.9, 35.2, 31.0; **MS** *m/z* (ES) $[M]^+$ 211.1.

Step-3: (3-(*tert*-butyl)-5-nitrophenyl)(methyl)sulfane (32): To a solution of 3-(*tert*-butyl)-5-nitrobenzenethiol (210 mg, 1.0 mmol) in EtOH (5 mL) NaOH (48 mg, 1.2 mmol) was added and the mixture was stirred at RT for 2 h. Methyl iodide (69 µL, 1.1

mmol) was added and the mixture was left to react overnight. The reaction was partitioned between water and AcOEt, extracted with AcOEt (2 × 10 mL), and the combined organic layers were washed with brine (1 × 15 mL), dried with $MgSO_4$ and condensed. The crude was purified by flash column chromatography (gradient hexane: AcOEt; 5:1 to 3:1) to give the desired product as a colourless oil (220 mg, 98%). **^{1}H-NMR** (300 MHz, $CDCl_3$) δ 7.92 (app. t, *J* = 1.8 Hz, 1H), 7.79 (app. t, *J* = 1.8 Hz, 1H), 7.48 (app. t, *J* = 1.8 Hz, 1H), 2.49 (s, 3H), 1.28 (s, 9H).

Step-4: 1-(*tert*-butyl)-3-(methylsulfonyl)-5-nitrobenzene (33): To a solution of (3-(*tert*-butyl)-5-nitrophenyl)(methyl)sulfane (0.42 g, 1.88 mmol) in CH_2Cl_2 (4 mL) at 0 °C *m*CPBA (1.10 g, 4.70 mmol) was added in one portion at room temperature. The mixture was left to warm up to room temperature and react for 2 h. Upon complete consumption of the starting material, the mixture was washed with $NaHCO_3$ (2 × 10 mL) and brine (10 mL), dried with $MgSO_4$ and condensed. The crude was purified by flash column chromatography (gradient hexane: AcOEt 4:1 to 2:1) to give the desired product as a white solid (333 mg, 73%). **^{1}H-NMR** (300 MHz, $CDCl_3$) δ 8.64-8.58 (m, 1H), 8.52 (app. t, *J* = 1.9 Hz, 1H), 8.28 (app. t, *J* = 1.9 Hz, 1H), 3.16 (s, 3H), 1.44 (s, 9H).

Step-5: 3-(*tert*-butyl)-5-(methylsulfonyl)aniline (34): A solution of 1-(*tert*-butyl)-3-(methylsulfonyl)-5-nitrobenzene (333 mg, 1.3 mmol) and palladium on carbon (10 mol%) in MeOH (6 mL) was stirred overnight under 5 atm of hydrogen. The mixture was thereafter filtered through celite, solvents were evaporated and the crude was purified by flash column chromatography (gradient hexane: AcOEt 4:1 to 2:1) to give the desired product as a white solid (230 mg, 76%). **^{1}H-NMR** (300 MHz, $CDCl_3$) δ 7.31 (app. t, *J* = 1.6 Hz, 1H), 7.05 (dd, *J* = 2.1, 1.7 Hz, 1H), 6.95 – 6.93 (m, 1H), 4.02 (s, 1H), 3.04 (s, 3H), 1.32 (s, 9H); **MS** *m/z* (ES) $[MH]^+$ 228.1.

Step-6: (*S*)-2-(3-aminopiperidin-1-yl)-4-((3-(tert-butyl)-5-(methylsulfonyl)phenyl)-amino) pyrimidine-5-carboxamide (16): Prepared in analogous manner to **9** using 3-(*tert*-butyl)-5-(methylsulfonyl)aniline. (32 mg, 10%). **^{1}H-NMR** (400 MHz, MeOD-d_4) δ 8.79 (s, 1H), 8.62 (s, 1H), 7.68 (app. t, J = 1.6 Hz, 1H), 7.55 (s, 1H), 4.71 (s, 1H), 4.38 (d, J = 11.8 Hz, 1H), 3.60-3.36 (m, 3H), 3.21 (s, 3H), 2.21 (d, J = 4.3 Hz, 1H), 1.93 (dd, J = 10.3, 5.0 Hz, 1H), 1.86-1.65 (m, 2H), 1.40 (s, 9H); **HRMS** (ES-TOF): *m/z* calcd. for $C_{21}H_{30}N_6O_3S$: 447.2178, found 447.2174 $[M+H]^+$.

(*S*)-2-(3-aminopiperidin-1-yl)-4-((5-(2-cyanopropan-2-yl)-[1,1'-biphenyl]-3-yl)amino)pyrimidine -5-carboxamide hydrochloride (17)

Step-1: *N*,*N*-dibenzyl-3,5-dibromoaniline (35): To 3,5-dibromoaniline (2.50 g, 9.96 mmol), potassium carbonate (4.13 g, 29.88 mmol) and benzyl bromide (3.55 mL, 29.89 mmol) was added MeCN (40 mL). The mixture was heated to reflux and left to stir overnight. After allowing the mixture to cool to RT, MeCN was removed under reduced pressure and AcOEt (60 mL) was added. The organic solution washed with water (3 × 50 mL), dried over $MgSO_4$, filtered and concentrated under reduced pressure to give the crude product, which was purified first by flash column chromatography (95:5 hexane:AcOEt) and then by recrystallisation from boiling hot hexane with a small amount of AcOEt (filtered while hot and left to cool) to give the title compound as a white solid (3.13 g, 73%). **^{1}H-NMR** (400 MHz, $CDCl_3$) δ 7.35 (app. t, J = 7.2 Hz, 4H), 7.31-7.25 (m, 2H), 7.19 (d, J = 7.6 Hz, 4H), 6.97 (s, 1H), 6.79 (s, 2H), 4.59 (s, 4H); **LC-MS** *m/z* (ES+) $(M+H)^+$ 431.8; t_R = 3.24 min. HPLC Method 3 (Acid).

Step-2: 2-(3-bromo-5-(dibenzylamino)phenyl)-2-methylpropanenitrile (37): . *N*,*N*-dibenzyl-3,5-dibromoaniline **51** (1.00 g, 2.32 mmol), Xantphos (0.16 g, 0.28 mmol), $Pd_2allyl_2Cl_2$ (0.04 g, 4 mol%) and potassium 2-cyano-2-methylpropanoate (0.84 g, 5.55 mmol) were added to a pressure vessel which was flushed with N_2 through a septum for 15 min. Mesitylene (5.5 mL) was introduced, the septum quickly replaced with a screwcap and the mixture stirred vigorously for 5 min at RT. The flask was lowered into an oil bath pre-heated to 140 ºC and left to stir vigorously overnight. Following cooling, the crude reaction mixture was transferred to a round bottomed flask with the aid of AcOEt (20 mL) and concentrated under reduced pressure. The resulting residue was purified by flash column chromatography on silica (gradient hexane, then 7:1 hexane: AcOEt followed by 6:1 and finally 5:1) to give:

- **2,2'-(5-(dibenzylamino)-1,3-phenylene)bis(2-methylpropanenitrile) (36):** Isolated as a light-yellow oil which solidified on standing (0.50 g, 53%). **^{1}H-NMR** (400 MHz, $CDCl_3$) δ 7.34 (*app* t, *J* = 7.6 Hz, 4H), 7.31-7.22 (m, 6H), 6.83 (s, 1H), 6.75 (d, *J* = 2.0 Hz, 2H), 4.70 (s, 4H), 1.60 (s, 12H). **LC-MS** *m/z* (ES+) $(M+H)^+$ 408.3; t_R = 2.88 min. HPLC Method 3 (Acid).
- **2-(3-bromo-5-(dibenzylamino)phenyl)-2-methylpropanenitrile (37):** Isolated as a light-yellow oil which solidified on standing (0.20 g, 20%). **^{1}H-NMR** (400 MHz, $CDCl_3$) δ 7.40-7.33 (m, 4H), 7.32–7.23 (m, 6H), 6.90 (app. t, *J* = 1.6 Hz, 1H), 6.85 (dd, *J* = 2.4, 1.6 Hz, 1H), 6.73 (app. t, *J* = 2.0 Hz, 1H), 4.67 (s, 4H), 1.58 (s, 6H); **LC-MS** *m/z* $(M+H)^+$ (ES^+) 419.3, 421.2; t_R = 3.14 min. HPLC Method 2 (Base).

Step-3: 2-(5-(dibenzylamino)-[1,1'-biphenyl]-3-yl)-2-methylpropanenitrile (39) A stirred solution of potassium carbonate (0.20 g, 1.44 mmol), phenyl-4,4,5,5-tetramethyl-1,3,2-dioxaborolane (0.15 g, 0.71 mmol) and 2-(3-bromo-5-(dibenzylamino)phenyl)-2-methylpropanenitrile **53** (0.20 g, 0.48 mmol) in 1,4-dioxane (8 mL) and water (2 mL) was purged with nitrogen for 10 min. $PdCl_2(PPh_3)_2$ (34 mg, 0.05 mmol) was added and purging was continued for a further 10 min. The reaction was then heated 100 °C and stirred under nitrogen for 1 h. Upon cooling, the solution was diluted with water (20 mL) and extracted with ethyl acetate (3 × 20 mL). The combined organic layers were dried over $MgSO_4$, filtered and concentrated under vacuum. The crude product was purified by chromatography on silica gel (20% AcOEt in hexane) to afford the titled product (0.14 g, 74%). **^{1}H-NMR** (400 MHz, $CDCl_3$) δ 7.52-7.44 (m, 2H), 7.44-7.25 (m, 13H), 7.02 (d, *J* = 1.5 Hz, 1H), 6.92 (app. t, *J* = 1.9 Hz, 1H), 6.82 (app. t, *J* = 2.1 Hz, 1H), 4.75 (s, 4H), 1.66 (s, 6H); **LC-MS** *m/z* $(M+H)^+$ (ES^+) 417.3; t_R = 3.14 min. HPLC Method 2 (Base).

Step-4: 2-(5-amino-[1,1'-biphenyl]-3-yl)-2-methylpropanenitrile (40): 2-(5-(dibenzylamino)-[1,1'-biphenyl]-3-yl)-2-methylpropanenitrile **54** (0.14 g, 0.34 mmol) was introduced to a flask which was flushed with N_2 for 10 min. $Pd(OH)_2$ (0.04 g, 10-20% Pd basis), CH_2Cl_2 (3.0 mL) and finally MeOH (3.0 mL) were added and the flask purged with H_2. The mixture was left to stir vigorously at RT for 1 h after which the flask was opened to the air and the mixture filtered through a pad of Celite® under reduced pressure. The cake was washed with additional MeOH (30 mL) and CH_2Cl_2 (30 mL), the filtrate concentrated under reduced pressure and the crude product purified by flash column chromatography on silica (20% AcOEt in hexane) to give the title compound as a colourless oil (60 mg, 88%). **^{1}H-NMR** (400 MHz, $CDCl_3$) δ 7.61-7.54 (m, 2H), 7.51-7.42 (m, 2H), 7.41-7.35 (m, 1H), 7.05 (app. t, *J* =

1.6 Hz, 1H), 6.86 (app. t, *J* = 1.8 Hz, 1H), 6.82 (app. t, *J* = 2.0 Hz, 1H), 1.77 (s, 6H); **LC-MS** *m/z* $(M+H)^+$ (ES^+) 237.2; t_R = 2.42 min. HPLC Method 2 (Base).

(*S*)-2-(3-aminopiperidin-1-yl)-4-((5-(2-cyanopropan-2-yl)-[1,1'-biphenyl]-3-yl)amino) pyrimidine -5-carboxamide hydrochloride (20): Compound **17** was prepared in analogous manner to **9** using 2-(5-amino-[1,1'-biphenyl]-3-yl)-2-methylpropanenitrile **40** and isolated as HCl salt (30 mg, 73%). **^{1}H-NMR** (400 MHz, MeOD-d_4) δ 8.61 (s, 1H), 8.04 (br. s, 1H), 7.72 (br. s, 1H), 7.70-7.66 (m, 2H), 7.62 (app. t, *J* = 1.7 Hz, 1H), 7.54-7.49 (m, 2H), 7.46-7.39 (m, 1H), 4.42 (app. dd, *J* = 14.0, 3.7 Hz, 1H), 4.08 (br. s, 1H), 3.82 (br. s, 1H), 3.69-3.60 (m, 1H), 3.57-3.48 (m, 1H), 2.27-2.14 (m, 1H), 2.05-1.94 (m, 1H), 1.88-1.79 (m, 8H); **LC-MS** *m/z* $(M+H)^+$ (ES^+) 456.3; t_R = 2.23 min. HPLC Method 2 (Base); **HRMS** (ES-TOF): *m/z* calcd. for $C_{26}H_{30}N_7O$: 456.2506, found 456.2506 $[M+H]^+$.

(*S*)-2-(3-aminopiperidin-1-yl)-4-((3,5-bis(2-cyanopropan-2-yl)phenyl)amino)pyrimidine-5- carboxamide hydrochloride (18)

Step-1: 2,2'-(5-amino-1,3-phenylene)bis(2-methylpropanenitrile) (38): 2,2'-(5-(dibenzylamino)-1,3-phenylene)bis(2-methylpropanenitrile) **36** (3.05 g, 7.48 mmol) was introduced to a flask which was flushed with N_2 for 10 min. $Pd(OH)_2$ (1.05 g, 10-20% Pd basis), CH_2Cl_2 (8.0 mL) and finally MeOH (30 mL) were added and the flask purged with H_2. The mixture was left to stir vigorously at RT for 3 h after which the flask was opened to the air and the mixture filtered through a pad of Celite® under reduced pressure. The cake was washed with additional MeOH (30 mL) and CH_2Cl_2 (30 mL), the filtrate concentrated under reduced pressure and the crude product purified by flash column chromatography on silica (1:1 hexane: AcOEt) to give the title compound as a light-yellow oil which slowly solidified on standing (1.68 g,

98%). **^{1}H-NMR** (400 MHz, $CDCl_3$) δ 6.85 (t, *J* = 2.0 Hz, 1H), 6.73 (d, *J* = 2.4 Hz, 1H), 3.36 – 2.78 (br s, 2H), 1.70 (s, 12H); **LC-MS** *m/z* (ES+) $(M+H)^+$ 228.2; t_R = 2.15 min. HPLC Method 3 (Acid).

Step-2: (*S*)-2-(3-aminopiperidin-1-yl)-4-((3,5-bis(2-cyanopropan-2-yl)phenyl)amino)pyrimidine-5-carboxamide hydrochloride (18): 2,2'-(5-amino-1,3-phenylene)bis(2-methylpropanenitrile) **38** (0.76 g, 3.36 mmol), 2,4-dichloropyrimidine-5-carboxamide (0.82 g, 4.28 mmol), triethylamine (1.01 mL, 7.25 mmol) were dissolved in anhydrous dioxane (35 mL). The mixture was heated at 50 ºC for 3 h and then left to cool to RT. Additional 2,4-dichloropyrimidine-5-carboxamide (0.06 g, 0.32 mmol) and triethylamine (0.09 mL, 0.65 mmol) were added and the mixture heated to 50 ºC for a further 1.5 h. The reaction mixture was allowed to cool to RT, and *tert*-butyl (*S*)-piperidin-3-ylcarbamate (0.73 g, 3.62 mmol) and triethylamine (1.01 mL, 7.25 mmol) were added and the reaction mixture heated at 50 ºC for 75 min. AcOEt (60 mL) was added and the solution washed sequentially with water (5 × 30 mL) and brine (30 mL). The organic phase was dried over $MgSO_4$, filtered and concentrated under reduced pressure to give the crude product from two displacements which was purified by flash column chromatography (gradient 1:2 hexane: AcOEt to 1:3) to give the product from two displacements (1.30 g, 71%). Dioxane (30 mL) was added followed by the drop-wise addition of 4M HCl in dioxane (15 mL) and the reaction mixture was stirred at RT for 24 h. Hexane (30 mL) was added and the solid filtered and triturated with Et_2O to remove residual dioxane. The resulting solid was filtered and dried to give the hydrochloride salt of the title compound as a light-yellow powder (1.12 g, 98%). **m.p.** 232-233 ºC; **^{1}H-NMR** (400 MHz, MeOD-d_4) δ 8.60 (s, 1H), 7.83 (d, *J* = 1.6 Hz, 2H), 7.50 (t, *J* = 1.6 Hz, 1H), 4.39 (dd, *J* = 13.6, 3.2 Hz, 1H), 4.14-3.95 (m, 1H), 3.89-3.77 (m, 1H), 3.68-3.62 (m,

1H), 3.57-3.49 (m, 1H), 2.23-2.13 (m, 1H), 2.07-1.95 (m, 1H), 1.89-1.80 (m, 1H), 1.79 (s, 12H). **^{13}C-NMR** (126 MHz, MeOD-d_4) δ 167.2, 159.1, 152.6, 145.0, 143.9, 137.6, 124.1, 119.1, 118.6, 101.5, 46.4, 45.2, 37.3, 27.8, 27.1, 21.1; **LC-MS** *m/z* (ES+) $(M+H)^+$ 447.0; t_R = 1.91 min. HPLC Method 3 (Acid); **HRMS** (ES-TOF): *m/z* calcd. for $C_{24}H_{31}N_8O$: 447.2615, found 447.2636 $[M+H]^+$.

(*S*)-2-(3-aminopiperidin-1-yl)-4-((2,6-diisopropylpyridin-4-yl)amino)pyrimidine-5-carboxamide (19)

Step-1: 2,6-di(prop-1-en-2-yl)pyridin-4-amine: A stirred solution of sodium bicarbonate (0.37 g, 4.37 mmol), 4,4,5,5-tetramethyl-2-(prop-1-en-2-yl)-1,3,2-dioxaborolane (0.93 mL, 4.96 mmol) and 2,6-dibromopyridin-4-amine (0.50 g, 1.99 mmol) in 1,4-dioxane (7 mL) and water (3 mL) was purged with nitrogen for 10 min. $PdCl_2$dppf (0.15 g, 0.20 mmol) was added and purging was continued for a further 10 min. The reaction was then heated 90 °C and stirred under nitrogen for 4 h. Upon cooling, the solution was diluted with water (20 mL) and extracted with ethyl acetate (3 × 20 mL). The combined organic layers were dried over $MgSO_4$, filtered and concentrated under vacuum. The crude product was purified by chromatography on silica gel (gradient 0-50% AcOEt/*iso*-hexane) to afford 2,6-di(prop-1-en-2-yl)pyridin-4-amine. (0.20 g, 54%); **LC-MS** *m/z* $(M+H)^+$ (ES^+) 175.2; t_R = 0.62 min. HPLC Method 2

Step-2: 2,6-diisopropylpyridin-4-amine (28): A solution of 2,6-di(prop-1-en-2-yl)pyridin-4-amine (0.20 g, 1.15 mmol) in methanol (4 mL) was hydrogenated in an H-Cube (10% Pd/C, 30×4 mm, Full hydrogen, 40 ºC, 1 mL/min) and concentrated under vacuum to afford 2,6-diisopropylpyridin-4-amine. (0.15 g, 75%). **LC-MS** *m/z* $(M+H)^+$ (ES^+) 179.2; t_R = 1.13 min. HPLC Method 4.

Step-3: (*S*)-2-(3-aminopiperidin-1-yl)-4-((2,6-diisopropylpyridin-4-yl)amino)pyrimidine-5-carboxamide (19): To a stirred solution of 2,4-dichloropyrimidine-5-carboxamide (0.97 g, 5.02 mmol) in 1,4-dioxane (20 mL) was added 2,6-diisopropylpyridin-4-amine **38** (0.69 g, 3.86 mmol) and DIPEA (1.35 mL, 7.73 mmol). The reaction was heated to 110 ºC and stirred for 7 h. The mixture was allowed to cool and concentrated under vacuum. The crude product was purified by chromatography on silica gel (0-2% (0.7 M Ammonia/MeOH):CH_2Cl_2) to afford 2-chloro-4-((2,6-diisopropylpyridin-4-yl)amino)pyrimidine-5-carboxamide. (0.91 g, 67%). **^{1}H-NMR** (500 MHz, DMSO-d_6) δ 11.66 (s, 1H), 8.86 (s, 1H), 8.50 (s, 1H), 8.04 (s, 1H), 7.40 (s, 2H), 2.95 (sept, 2H, J = 6.9 Hz), 1.24 (d, 12H, J = 6.9 Hz); **LC-MS** *m/z* $(M+H)^+$ (ES^+) 334.2; t_R = 2.26 min. HPLC Method 4.

To a stirred solution of 2-chloro-4-((2,6-diisopropylpyridin-4-yl)amino)pyrimidine-5-carboxamide (0.91 g, 2.70 mmol) in 1,4-dioxane (20 mL) was added (*S*)-*tert*-butyl piperidin-3-ylcarbamate (0.57 g, 2.83 mmol) and DIPEA (0.49 mL, 2.83 mmol). The reaction was heated to 90 °C and stirred for 30 min, then allowed to cool and concentrated under vacuum. The crude product was purified by chromatography on silica gel (0-2% (0.7 M Ammonia/MeOH) :CH_2Cl_2) to afford (*S*)-*tert*-butyl (1-(5-carbamoyl-4-((2,6-diisopropylpyridin-4-yl)amino)pyrimidin-2-yl)piperidin-3-yl)carbamate. (1.19 g, 88%). **LC-MS** *m/z* $(M+H)^+$ (ES^+) 498.5; t_R = 2.49 min. HPLC Method 4.

To a stirred solution of (*S*)-*tert*-butyl (1-(5-carbamoyl-4-((2,6-diisopropylpyridin-4-yl)amino)pyrimidin-2-yl)piperidin-3-yl)carbamate (1.19 g, 2.391 mmol) in 1,4-dioxane (10 mL) was added 4M hydrochloric acid in dioxane (11.96 mL, 47.8 mmol) and the reaction was stirred at RT for 4 h. The reaction mixture was then concentrated under vacuum. The residue was diluted in MeOH (0.20 mL) and loaded onto a SCX

cartridge, washing with MeOH (3 column volumes) and eluting with 1% NH_3 MeOH (3 column volumes). The ammonical MeOH was removed under reduced pressure to give the titled compound as a white solid (0.85 g, 78%). **m.p.** 225-226 ºC; **^{1}H-NMR** (500 MHz, MeOD-d_4) δ 8.59 (s, 1H), 7.44 (s, 2H), 4.63 (dd, J = 12.7, 4.0 Hz, 1H), 4.58-4.50 (m, 1H), 3.22 (ddd, J = 13.6, 10.8, 3.2 Hz, 1H), 3.09-2.95 (m, 3H), 2.88-2.77 (m, 1H), 2.08-2.00 (m, 1H), 1.88-1.78 (m, 1H), 1.65-1.52 (m, 1H), 1.51-1.40 (m, 1H), 1.30 (dd, J = 7.0, 2.7 Hz, 12H); **^{13}C-NMR** (126 MHz, Methanol-d_4) δ 170.3, 167.3, 161.0, 159.8, 158.2, 147.7, 108.0, 98.5, 51.0, 44.2, 35.9, 32.5, 23.3, 21.8; **LC-MS** *m/z* $(M+H)^+$ (ES^+) 398.3; t_R = 1.79 min. HPLC Method 4; **HRMS** (ES-TOF): *m/z* calcd. for $C_{21}H_{31}N_7ONa$: 420.2482, found 420.2473 $[M+Na]^+$.

CONCLUSION

We have identified highly potent and selective *in vitro* and *in vivo* probes of CaMK1 kinases through a structure-based-design approach. These probes should be of utility to researchers working on CaMK1 biology *in vitro*, or who wish to investigate the effects of targeting the peripheral function of CaMK1 enzymes.

CORRESPONDING AUTHOR

Sam Butterworth: sam.butterworth@manchester.ac.uk

ORCID: 0000-0002-6549-3753

AUTHOR CONTRIBUTIONS

Compounds were designed and synthesised by C.F., A.A., D.K., L.H., G.G., A.C., H.V.N., D.H.J., M.G.S., A.V.R., B.S., G.P.I., C.J.H., P.M.F. and S.B. *In vitro* biology studies were designed and/or performed by M.L., S.R., C.B., J.K., P.G., V.N., J.M.,

A.C.R., A.K., C.K., M.O., S.K., and F.B. Crystal structure analysis was performed by F.S. and A.K. *In vivo* DIO mice studies were designed by S.B., B.L., C.J.W. S.C.C. and S.P.V. The data obtained were interpreted by all authors. All authors have given approval to the final version of the manuscript.

ASSOCIATED CONTENT

Supporting Information

Experimental data from X-Ray crystal structures, experimental details for DIO mouse OGTT study and full Eurofins Discover X profiles (pdf). Molecular SMILES strings and in vitro results including number of replicates and standard deviation values (csv).

Accession Codes

X-ray coordinates and structures factors have been deposited in the Protein Data Bank under the following accession codes; Compound **8**, PDB6T6F; Compound **18**, PDB6T28; Compound **19**, PDB6T29. Authors will release the atomic coordinates upon article publication.

NOTES

The authors declare no competing financial interests. C.J.W. is funded by the NIHR Birmingham Biomedical Research Centre at the University Hospitals Birmingham NHS Foundation Trust and the University of Birmingham. This paper presents independent research supported by the NIHR Birmingham Biomedical Research Centre at the University Hospitals Birmingham NHS Foundation Trust and the University of Birmingham. The views expressed are those of the author(s) and not necessarily those of the NHS, the NIHR or the Department of Health and Social Care.

In vivo studies were conducted in the UK in accordance with the Animal Ethical Review Group, University of Birmingham and UK Home Office legislation, the Animal Scientific Procedures Act 1986, under Home Office project licences 70/8420 (Saretius, PK studies) and 30/3208 (RenaSci, efficacy studies in DIO mice).

FUNDING SOURCES

This work was supported by the Wellcome Trust [103022], [202708] and MRC [MC_PC_15032].

ACKNOWLEDGEMENTS

KINOME*scan*® TREE*spot*™ images generated using TREE*spot*™ Software Tool and reprinted with permission from KINOME*scan*®, a division of DiscoveRx Corporation, © DISCOVERX CORPORATION 2010. DIO mice studies were conducted by RenaSci (Nottingham,UK). Marvin, Calculator Plugins and JChem Base were used for drawing, displaying and characterising chemical structures, structure searching and chemical database access and management, ChemAxon (http://www.chemaxon.com).

ABBREVIATIONS

CaMK1, calmodulin-dependent kinase; GWAS, genome-wide association studies; FOXA1, Hepatocyte nuclear factor 3-alpha; siRNA, small interfering ribonucleic acid; CRTC2/TORC2, CREB regulated transcription coactivator 2; TNBC, triple-negative breast cancer; SYK, Spleen tyrosine kinase; DIO, diet-induced obese; OGTT, oral glucose tolerance test.

REFERENCES

(1) Parkinson, H.; Kapushesky, M.; Shojatalab, M.; Abeygunawardena, N.; Coulson, R.; Farne, A.; Holloway, E.; Kolesnykov, N.; Lilja, P.; Lukk, M.; Mani, R.; Rayner, T; Sharma, A.; William, E.; Sarkans, U.; Brazma, A. ArrayExpress--a Public Database of Microarray Experiments and Gene Expression Profiles. *Nucleic Acids Res.* **2007**, *35* (Database issue), D747-750.

(2) Wayman, G. A.; Lee, Y.-S.; Tokumitsu, H.; Silva, A. J.; Silva, A.; Soderling, T. R. Calmodulin-Kinases: Modulators of Neuronal Development and Plasticity. *Neuron* **2008**, *59* (6), 914–931.

(3) Zeggini, E.; Scott, L. J.; Saxena, R.; Voight, B. F.; Marchini, J. L.; Hu, T.; de Bakker, P. I.; Abecasis, G. R.; Almgren, P.; Andersen, G.; Ardlie, K.; Boström, K.B.; Bergman, R.N.; Bonnycastle, L.L.; Borch-Johnsen, K.; Burtt, N.P.; Chen, H.; Chines, P.S.; Daly, M.J.; Deodhar, P.; Ding, C.J.; Doney, A.S.; Duren, W.L.; Elliott, K.S.; Erdos, M.R.; Frayling, T.M.; Freathy, R.M.; Gianniny, L.; Grallert, H.; Grarup, N.; Groves, C.J.; Guiducci, C.; Hansen, T.; Herder, C.; Hitman, G.A.; Hughes, T.E.; Isomaa, B.; Jackson, A.U.; Jørgensen, T.; Kong, A.; Kubalanza, K.; Kuruvilla, F.G.; Kuusisto, J.; Langenberg, C.; Lango, H.; Lauritzen, T.; Li, Y.; Lindgren, C.M.; Lyssenko, V.; Marvelle, A.F.; Meisinger, C.; Midthjell, K.; Mohlke, K.L.; Morken, M.A.; Morris, A.D.; Narisu, N.; Nilsson, P.; Owen, K.R.; Palmer, C.N.; Payne, F.; Perry, J.R.; Pettersen, E.; Platou, C.; Prokopenko, I.; Qi, L.; Qin, L.; Rayner, N.W.; Rees, M.; Roix, J.J.; Sandbaek, A.; Shields, B.; Sjögren, M.; Steinthorsdottir, V.; Stringham, H.M.; Swift, A.J.; Thorleifsson, G.; Thorsteinsdottir, U.; Timpson, N.J.; Tuomi, T.; Tuomilehto, J.; Walker, M.; Watanabe, R.M.; Weedon, M.N.; Willer, C.J; Wellcome Trust Case Control

Consortium.; Illig, T.; Hveem, K.; Hu, F.B.; Laakso, M.; Stefansson, K.; Pedersen, O.; Wareham, N.J.; Barroso, I.; Hattersley, A.T.; Collins, F.S.; Groop, L.; McCarthy, M.I.; Boehnke, M.; Altshuler, D.. Meta-Analysis of Genome-Wide Association Data and Large-Scale Replication Identifies Additional Susceptibility Loci for Type 2 Diabetes. *Nat. Genet.* **2008**, *40* (5), 638-645.

(4) Shu, X. O.; Long, J.; Cai, Q.; Qi, L.; Xiang, Y.-B.; Cho, Y. S.; Tai, E. S.; Li, X.; Lin, X.; Chow, W.-H.; Go, M.J.; Seielstad, M.; Bao, W.; Li, H.; Cornelis, M.C.; Yu, K.; Wen, W.; Shi, J.; Han, B.G.; Sim, X.L.; Liu, L.; Qi, Q.; Kim, H.L.; Ng, D.P.; Lee, J.Y.; Kim, Y.J.; Li, C.; Gao, Y.T.; Zheng, W.; Hu, F.B. Identification of New Genetic Risk Variants for Type 2 Diabetes. *PLoS Genet.* **2010**, *6* (9), e1001127.

(5) Kooner, J. S.; Saleheen, D.; Sim, X.; Sehmi, J.; Zhang, W.; Frossard, P.; Been, L. F.; Chia, K.-S.; Dimas, A. S.; Hassanali, N.; Jafar, T.; Jowett, J.B.; Li, X.; Radha, V.; Rees, S.D.; Takeuchi, F.; Young, R.; Aung, T.; Basit, A.; Chidambaram, M.; Das, D.; Grundberg, E.; Hedman, A.K.; Hydrie, Z.I.; Islam, M.; Khor, C.C.; Kowlessur, S.; Kristensen, M.M.; Liju, S.; Lim, W.Y.; Matthews, D.R.; Liu, J.; Morris, A.P.; Nica, A.C.; Pinidiyapathirage, J.M.; Prokopenko, I.; Rasheed, A.; Samuel, M.; Shah, N.; Shera, A.S.; Small, K.S.; Suo, C.; Wickremasinghe, A.R.; Wong, T.Y.; Yang, M.; Zhang, F; DIAbetes Genetics Replication And Meta-analysis (DIAGRAM) Consortium; MuTHER Consortium; Abecasis, G.R.; Barnett, A.H.; Caulfield, M.; Deloukas, P.; Frayling, T.M.; Froguel, P.; Kato, N.; Katulanda, P.; Kelly, M.A.; Liang, J.; Mohan, V.; Sanghera, D.K.; Scott, J.; Seielstad, M.; Zimmet, P.Z.; Elliott, P.; Teo, Y.Y.; McCarthy, M.I.; Danesh, J.; Tai, E.S.; Chambers, J.C. Genome-

Wide Association Study in Individuals of South Asian Ancestry Identifies Six New Type 2 Diabetes Susceptibility Loci. *Nat. Genet.* **2011**, *43* (10), 984–989.

(6) Morris, A. P.; Voight, B. F.; Teslovich, T. M.; Ferreira, T.; Segrè, A. V; Steinthorsdottir, V.; Strawbridge, R. J.; Khan, H.; Grallert, H.; Mahajan, A.; Prokopenko, I.; Kang, H.M.; Dina, C.; Esko, T.; Fraser, R.M.; Kanoni, S.; Kumar, A.; Lagou, V.; Langenberg, C.; Luan, J.; Lindgren, C.M.; Müller-Nurasyid, M.; Pechlivanis, S.; Rayner, N.W.; Scott, L.J.; Wiltshire, S.; Yengo, L.; Kinnunen, L.; Rossin, E.J.; Raychaudhuri, S.; Johnson, A.D.; Dimas, A.S.; Loos, R.J.; Vedantam, S.; Chen, H.; Florez, J.C.; Fox, C.; Liu, C.T.; Rybin, D.; Couper, D.J.; Kao, W.H.; Li, M.; Cornelis, M.C.; Kraft, P.; Sun, Q.; van, Dam, R.M.; Stringham, H.M.; Chines, P.S.; Fischer, K.; Fontanillas, P.; Holmen, O.L.; Hunt, S.E.; Jackson, A.U.; Kong, A.; Lawrence, R.; Meyer, J.; Perry, J.R.; Platou, C.G.; Potter, S.; Rehnberg, E.; Robertson, N.; Sivapalaratnam, S.; Stančáková A.; Stirrups, K.; Thorleifsson, G.; Tikkanen, E.; Wood, A.R.; Almgren, P.; Atalay, M.; Benediktsson, R.; Bonnycastle, L.L.; Burtt, N.; Carey, J.; Charpentier, G.; Crenshaw, A.T.; Doney, A.S.; Dorkhan, M.; Edkins, S.; Emilsson, V.; Eury, E.; Forsen, T.; Gertow, K.; Gigante, B.; Grant, G.B.; Groves, C.J.; Guiducci, C.; Herder, C.; Hreidarsson, A.B.; Hui, J.; James, A.; Jonsson, A.; Rathmann, W.; Klopp, N.; Kravic, J.; Krjutškov, K.; Langford, C.; Leander, K.; Lindholm, E.; Lobbens, S.; Männistö S.; Mirza, G.; Mühleisen, T.W.; Musk, B.; Parkin, M.; Rallidis, L.; Saramies, J.; Sennblad, B.; Shah, S.; Sigurðsson, G.; Silveira, A.; Steinbach, G.; Thorand, B.; Trakalo, J.; Veglia, F.; Wennauer, R.; Winckler, W.; Zabaneh, D.; Campbell, H.; van, Duijn, C.; Uitterlinden, A.G.; Hofman, A.; Sijbrands, E.; Abecasis, G.R.; Owen, K.R.; Zeggini, E.; Trip, M.D.; Forouhi, N.G.; Syvänen, A.C.; Eriksson, J.G.;

Peltonen, L.; Nöthen, M.M.; Balkau, B.; Palmer, C.N.; Lyssenko, V.; Tuomi, T.; Isomaa, B.; Hunter, D.J.; Qi, L; Wellcome Trust Case Control Consortium; Meta-Analyses of Glucose and Insulin-related traits Consortium (MAGIC) Investigators; Genetic, Investigation of ANthropometric, Traits (GIANT) Consortium; Asian Genetic Epidemiology Network–Type 2 Diabetes (AGEN-T2D) Consortium; South Asian Type 2 Diabetes (SAT2D) Consortium.; Shuldiner, A.R.; Roden M.; Barroso, I.; Wilsgaard, T.; Beilby, J.; Hovingh, K.; Price, J.F.; Wilson, J.F.; Rauramaa, R.; Lakka, T.A.; Lind, L.; Dedoussis, G.; Njølstad, I.; Pedersen, N.L.; Khaw, K.T.; Wareham, N.J.; Keinanen-Kiukaanniemi, S.M.; Saaristo, T.E.; Korpi-Hyövälti, E.; Saltevo, J.; Laakso, M.; Kuusisto, J.; Metspalu, A.; Collins, F.S.; Mohlke, K.L.; Bergman, R.N.; Tuomilehto, J.; Boehm, B.O.; Gieger, C.; Hveem, K.; Cauchi, S.; Froguel, P.; Baldassarre, D.; Tremoli, E.; Humphries, S.E.; Saleheen, D.; Danesh, J.; Ingelsson, E.; Ripatti, S.; Salomaa, V.; Erbel, R.; Jöckel, K.H.; Moebus, S.; Peters, A.; Illig, T.; de, Faire, U.; Hamsten, A.; Morris, A.D.; Donnelly, P.J.; Frayling, T.M.; Hattersley, A.T.; Boerwinkle, E.; Melander, O.; Kathiresan, S.; Nilsson, P.M.; Deloukas, P.; Thorsteinsdottir, U.; Groop, L.C.; Stefansson, K.; Hu, F.; Pankow, J.S.; Dupuis, J.; Meigs, J.B.; Altshuler, D.; Boehnke, M.; McCarthy, M.I; DIAbetes Genetics Replication And Meta-analysis (DIAGRAM) Consortium. Large-Scale Association Analysis Provides Insights into the Genetic Architecture and Pathophysiology of Type 2 Diabetes. *Nat. Genet.* **2012**, *44* (9), 981–990.

(7) Fogarty, M. P.; Cannon, M. E.; Vadlamudi, S.; Gaulton, K. J.; Mohlke, K. L. Identification of a Regulatory Variant That Binds FOXA1 and FOXA2 at the CDC123/CAMK1D Type 2 Diabetes GWAS Locus. *PLoS Genet.* **2014**, *10* (9),

e1004633.

(8) Haney, S.; Zhao, J.; Tiwari, S.; Eng, K.; Guey, L. T.; Tien, E. RNAi Screening in Primary Human Hepatocytes of Genes Implicated in Genome-Wide Association Studies for Roles in Type 2 Diabetes Identifies Roles for CAMK1D and CDKAL1, among Others, in Hepatic Glucose Regulation. *PLoS One* **2013**, *8* (6), e64946.

(9) Saberi, M.; Bjelica, D.; Schenk, S.; Imamura, T.; Bandyopadhyay, G.; Li, P.; Jadhar, V.; Vargeese, C.; Wang, W.; Bowman, K.; Zhang, Y.; Polisky, B.; Olefsky, J.M. Novel Liver-Specific TORC2 SiRNA Corrects Hyperglycemia in Rodent Models of Type 2 Diabetes. *Am. J. Physiol. Metab.* **2009**, *297* (5), E1137–E1146.

(10) Wang, Y.; Inoue, H.; Ravnskjaer, K.; Viste, K.; Miller, N.; Liu, Y.; Hedrick, S.; Vera, L.; Montminy, M. Targeted Disruption of the CREB Coactivator Crtc2 Increases Insulin Sensitivity. *Proc. Natl. Acad. Sci.* **2010**, *107* (7), 3087–3092.

(11) Erion, D. M.; Kotas, M. E.; McGlashon, J.; Yonemitsu, S.; Hsiao, J. J.; Nagai, Y.; Iwasaki, T.; Murray, S. F.; Bhanot, S.; Cline, G. W.; Samuel, V.T. CAMP-Responsive Element-Binding Protein (CREB)-Regulated Transcription Coactivator 2 (CRTC2) Promotes Glucagon Clearance and Hepatic Amino Acid Catabolism to Regulate Glucose Homeostasis. *J. Biol. Chem.* **2013**, *288* (22), 16167–16176.

(12) Loo, L. W. M.; Wang, Y.; Flynn, E. M.; Lund, M. J.; Bowles, E. J. A.; Buist, D. S. M.; Liff, J. M.; Flagg, E. W.; Coates, R. J.; Eley, J. W.; Hsu, L.; Porter, P.L. Genome-Wide Copy Number Alterations in Subtypes of Invasive Breast Cancers in Young White and African American Women. *Breast Cancer Res.*

Treat. **2011**, *127* (1), 297–308.

(13) Shavers, V. L.; Harlan, L. C.; Stevens, J. L. Racial/Ethnic Variation in Clinical Presentation, Treatment, and Survival among Breast Cancer Patients under Age 35. *Cancer* **2003**, *97* (1), 134–147.

(14) Bergamaschi, A.; Kim, Y. H.; Kwei, K. A.; La Choi, Y.; Bocanegra, M.; Langerød, A.; Han, W.; Noh, D.-Y.; Huntsman, D. G.; Jeffrey, S. S.; Børresen-Dale, A-L.; Pollack, J.R.. CAMK1D Amplification Implicated in Epithelial-Mesenchymal Transition in Basal-like Breast Cancer. *Mol. Oncol.* **2008**, *2* (4), 327–339.

(15) Yamada, T.; Suzuki, M.; Satoh, H.; Kihara-Negishi, F.; Nakano, H.; Oikawa, T. Effects of PU.1-Induced Mouse Calcium–Calmodulin-Dependent Kinase I-like Kinase (CKLiK) on Apoptosis of Murine Erythroleukemia Cells. *Exp. Cell Res.* **2004**, *294* (1), 39–50.

(16) Hisamichi, H.; Naito, R.; Toyoshima, A.; Kawano, N.; Ichikawa, A.; Orita, A.; Orita, M.; Hamada, N.; Takeuchi, M.; Ohta, M.; Tsukamoto, S-i. Synthetic Studies on Novel Syk Inhibitors. Part 1: Synthesis and Structure–Activity Relationships of Pyrimidine-5-Carboxamide Derivatives. *Bioorg. Med. Chem.* **2005**, *13* (16), 4936–4951.

(17) Liddle, J.; Atkinson, F. L.; Barker, M. D.; Carter, P. S.; Curtis, N. R.; Davis, R. P.; Douault, C.; Dickson, M. C.; Elwes, D.; Garton, N. S.; Gray M, Hayhow, T.G.; Hobbs, C.I.; Jones, E.; Leach, S.; Leavens, K.; Lewis, H.D.; McCleary, S.; Neu, M.; Patel, V.K.; Preston, A.G.; Ramirez-Molina, C.; Shipley, T.J.; Skone, P.A.; Smithers, N.; Somers, D.O.; Walker, A.L.; Watson, R.J.; Weingarten, G.G. Discovery of GSK143, a Highly Potent, Selective and Orally Efficacious Spleen Tyrosine Kinase Inhibitor. *Bioorg. Med. Chem. Lett.* **2011**,

21 (20), 6188–6194.

(18) Thoma, G.; Smith, A. B.; van Eis, M. J.; Vangrevelinghe, E.; Blanz, J.; Aichholz, R.; Littlewood-Evans, A.; Lee, C. C.; Liu, H.; Zerwes, H.-G. Discovery and Profiling of a Selective and Efficacious Syk Inhibitor. *J. Med. Chem.* **2015**, *58* (4), 1950–1963.

(19) Ellis, J. M.; Altman, M. D.; Bass, A.; Butcher, J. W.; Byford, A. J.; Donofrio, A.; Galloway, S.; Haidle, A. M.; Jewell, J.; Kelly, N.; Leccese, E.K.; Lee, S.; Maddess, M.; Miller, J.R.; Moy, L.Y.; Osimboni, E.; Otte, R.D.; Reddy, M.V.; Spencer, K.; Sun, B.; Vincent, S.H.; Ward, G.J.; Woo, G.H.; Yang, C.; Houshyar, H.; Northrup, A.B. Overcoming Mutagenicity and Ion Channel Activity: Optimization of Selective Spleen Tyrosine Kinase Inhibitors. *J. Med. Chem.* **2015**, *58* (4), 1929–1939.

(20) Gao, Y.; Davies, S. P.; Augustin, M.; Woodward, A.; Patel, U. A.; Kovelman, R.; Harvey, K. J. A Broad Activity Screen in Support of a Chemogenomic Map for Kinase Signalling Research and Drug Discovery. *Biochem. J.* **2013**, *451* (2), 313–328.

(21) Shang, R.; Ji, D.-S.; Chu, L.; Fu, Y.; Liu, L. Synthesis of α-Aryl Nitriles through Palladium-Catalyzed Decarboxylative Coupling of Cyanoacetate Salts with Aryl Halides and Triflates. *Angew. Chemie Int. Ed.* **2011**, *50* (19), 4470–4474.

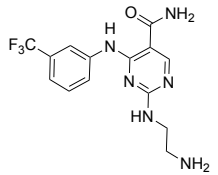

Literature SYK inhibitor

SYK IC_{50} = **7 nM**

CaMK1D IC_{50} = **436 nM**

Structure and T_m panel informed optimisation

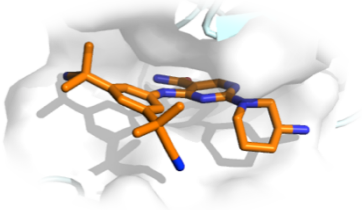

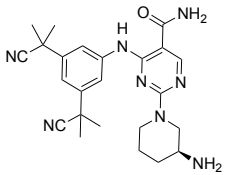

CaMK1 *in vivo* tool compounds

CaMK1D IC_{50} = **31 nM**

pCaMK1D cell assay IC_{50} = **8 nM**

>>150-fold selective over non-CaMK1 kinases

Active in DIO mouse model